THE EFFECT OF PERONEAL NERVE RELOCATION ON SKELETAL MUSCLE REGENERATION WITHIN AN EXTRACELLULAR MATRIX SEEDED WITH MESENCHYMAL STEM CELL POPULATIONS DERIVED FROM BONE MARROW AND ADIPOSE TISSUE

Matthew Timothy Tierney, B.S.

Presented to the Faculty of the Graduate School
of The University of Texas at Austin
in Partial Fulfillment
of the Requirements
for the Degree of

Master of Arts

The University of Texas at Austin
August 2009

THE EFFECT OF PERONEAL NERVE RELOCATION ON SKELETAL MUSCLE REGENERATION WITHIN AN EXTRACELLULAR MATRIX SEEDED WITH MESENCHYMAL STEM CELL POPULATIONS DERIVED FROM BONE MARROW AND ADIPOSE TISSUE

Approved by Supervising Committee:

_____

Roger P. Farrar

_____

Laura J. Suggs

DEDICATION

This work is dedicated to my family and all those who have helped me in my academic pursuits. I would like to give a special thank you to my parents, Tim and Luann Tierney, for their love and support over the years.

ACKNOWLEDGEMENTS

This work would not have been possible without the knowledge and patience of my advisor, Dr. Roger Farrar. He has been an excellent mentor, never without a valuable insight and always abundantly helpful. One simply could not wish for a friendlier supervisor. Many thanks to Dr. Laura Suggs, who took the time to be my second reader and generously gave me the benefit of her academic experience. Ed Merritt, David Hammers, Megan Cannon and Apurva Sarathy also reviewed this manuscript, helping me to bring focus and clarity to the text while rescuing me from error. I would like to thank Dr. Wes Thompson for his help in developing the surgical procedures used in this study, particularly the relocation of the peroneal nerve. His expertise in the field of molecular neurobiology was indispensable. Thanks to Tom Walters of the United States Institute of Surgical Research for his intellectual support during my time here as at the University of Texas at Austin. Everyone should have a friend as good and helpful and accommodating as Patty Coffman. Her kindness and assistance with every administrative task and favor asked was tremendous. Finally, I am indebted to all of my fellow graduate students: Ed Merritt, David Hammers, Daria Nedrie, Rohit Gohkale, Tae Joeng, Megan Cannon, Daniel Taylor, Apurva Sarathy and Melissa Merscham. You all were a tremendous help and have assisted me in numerous ways, and I've greatly enjoyed my time spent in our laboratory largely because of you. Thank you all very much.

THE EFFECT OF PERONEAL NERVE RELOCATION ON SKELETAL MUSCLE REGENERATION WITHIN AN EXTRACELLULAR MATRIX SEEDED WITH MESENCHYMAL STEM CELL POPULATIONS DERIVED FROM BONE MARROW AND ADIPOSE TISSUE

Matthew Timothy Tierney, M.A.
The University of Texas at Austin, 2009
Supervisor: Roger P. Farrar

Despite the normally robust regenerative capacity of muscle tissue, extensive soft tissue damage often results in a functional loss that cannot be restored using classic reconstruction techniques. Although implanted biomaterials are capable of mechanically transmitting force generated from the remaining tissue, cellular repopulation, reinnervation and revascularization of the injured area is necessary to achieve complete functional restoration. Using an *in vivo* tissue engineering model, a 1.0 x 1.0 cm portion of the lateral gastrocnemius (LGAS) of Lewis rats was removed and replaced with a muscle-derived extracellular matrix (ECM). Constructs were seeded with bone marrow-derived (BMSCs) or adipose-derived stem cells (ADSCs) and the peroneal nerve was relocated over the implanted ECM. Creation of the defect resulted in a functional impairment of the LGAS, only capable of producing 85.1 ± 4.1% of the force generated in the contralateral LGAS following ECM implantation. A significant increase in specific tension (SPo) was seen in all groups following the nerve relocation procedure when compared to their corresponding cellular treatment without nerve relocation ($p < 0.05$). Histological quantification revealed significant increases in cellular content and blood vessel density in the top and bottom regions of ECM implants seeded with BMSCs ($p < 0.05$). The nerve relocation procedure significantly increased these same variables within the middle region of the ECM when compared to all groups lacking this treatment ($p < 0.05$). The presence of regenerating myofibers was immunofluorescently confirmed using antibodies against desmin, myosin heavy

chain and laminin, while their developmental state was substantiated by the presence of central nuclei. These data corroborate a therapeutic effect of BMSCs on skeletal muscle regeneration within the ECM implant that was not seen following ADSC injection. Furthermore, the nerve relocation procedure stimulated an increased cellular and vascular growth within the middle region of the construct, likely the cause of improved functional output.

TABLE OF CONTENTS

LIST OF FIGURES

INTRODUCTION

Traumatic injury to the extremities results in extensive soft tissue damage and functional loss to the wounded limb. It may also lead to a loss of muscle mass and consequent change in aesthetic appearance that is undesirable to the patient. Surgical options to repair a large muscle defect are limited. Autologous tissue transfer has been shown to restore some function to the damaged area but risks donor site morbidity, results in functional loss at the donor site and is only applicable to small muscle defects (Tu et al. 2008). Alternatively, replacement of loss tissue with a biocompatible scaffold might be able to return both mass and function to the injured site are needed.

Simply implanting an extracellular matrix (ECM) itself does not restore function but is capable of supporting myofiber ingrowth (Merritt et al. 2009). Certainly, cellular repopulation is necessary to restore functionality to the defected area. Selection of a cellular population should be based upon ease of acquisition, clinical relevance, immunogenicity, proliferative capacity and myogenic potential. Recently, somatic mesenchymal stem cells (MSCs) have generated a great deal of excitement in the scientific community. These multipotent progenitor cells are obtained directly from patients, eliminating the immune response associated with allogenic cells. First derived from bone marrow, they expand rapidly in culture (Friedenstein et al. 1970) and are capable of differentiation into functional myofibers (Ferrari et al. 1998). Remarkably, MSCs have been shown to migrate to the injury site and mediate the postnatal regenerative process either by differentiating into tissue-specific cell phenotypes (Dezawa et al. 2005, Palermo et al. 2005, Collins et al. 2005) or by creating a milieu that increases the capacity of the endogenous cells to repair the tissue (Ohtaki et al. 2008, Gupta et al. 2007, Prockop 2009).

While their therapeutic effects *in vivo* are well documented, bone marrow-derived stem cells (BMSCs) require invasive extraction procedures that carry a small but significant risk of post-operative infection and anemia. Furthermore, the cells must be expanded in culture to achieve a clinically relevant cell count, creating a time gap between cell acquisition and transplantation. Adipose tissue also contains a heterogeneous stromal cell population (Zuk et al. 2001) and is easily obtained via liposuction. A larger quantity of adipose-derived stem cells (ADSCs) can be retrieved at a greater concentration than BMSCs (Padoin et al. 2008) and may be sufficient for immediate isolation and transplantation back into the damaged or diseased tissue.

Additionally, both innervation and vascularization of the construct is critical to the outcome of muscle regeneration. Loss of skeletal muscle tissue will invariably include injury to the nervous tissue and vasculature of the injured muscle. If the newly regenerated myofibers cannot be stimulated to contract, it will undergo a repeated cycle of growth and decay, eventually resulting in continued impairment of the muscle's functional capacity (Borisov et al. 2001, Borisov et al. 2005). Similarly, continued regeneration and terminal differentiation of neomyofibers is likely prevented when contained within an avascular, and therefore hypoxic, area (Li et al. 2007). Interestingly, the regeneration potential of these two systems is related as a well-vascularized construct has been shown to enhance nerve regeneration (Hobson et al. 1997) while prolonged denervation stimulates the degeneration of the associated vasculature (Borisov et al. 2001).

The relocation of the peroneal nerve (Jansen et al. 1973) may be able to benefit the regenerative process via neurotization and the formation of new ectopic motor endplates, resulting in the continued survival and functional contribution of regenerating myofibers (Payne & Brushart 1997). In addition, the presentation of neurotrophins has been shown to play a role in regulating skeletal muscle

regeneration and repair. Primarily thought to promote neuronal survival and axonal outgrowth, both neural growth factor (NGF) and brain-derived neurotrophic factor (BDNF) are synthesized and secreted by sympathetic neurons of the periphery (Hasan et al. 2003). They normally act on tyrosine kinase (Trk) or p75 neurotrophin ($p75^{NTR}$) receptors via an autocrine/paracrine signaling mechanism, but may induce greater activity in cells expressing both receptors. Activated $p75^{NTR}$ affects the conformation of the Trk receptor, allowing for the formation of high-affinity binding sites for neurotrophins, especially NGF (Deponti et al. 2009). Indeed, NGF is highly expressed in regenerating skeletal muscle fibers following injury (Lavasani et al. 2006) and has been shown to stimulate the fusion of regenerating myoblasts and aids in the development of mature sarcomeres (Deponti et al. 2009). Conversely, presentation of an NGF antagonist delays muscle regeneration in part by decreasing the number of regenerating myofibers.

To create a functioning muscle construct, we utilized an *in vivo* tissue engineering model in Lewis rats. A 1.0 x 1.0 cm portion of the lateral gastrocnemius (LGAS) was removed, replaced with a muscle-derived extracellular matrix (ECM) and supplemented with either bone marrow-derived or adipose-derived stem cells. It was the intent of this investigation to ascertain, through morphological, functional and histological analyses, the efficacy of each cell population in repopulating and restoring function to the construct, as well as to determine the effect of relocating the peroneal nerve to the surface of the ECM.

LITERATURE REVIEW

Skeletal Muscle Trauma

Orthopedic injuries to the extremities comprise a majority of combat injuries seen in recent United States military conflicts (Owens et al. 2006, Lin et al. 2004). Recent reports from *Operation Iraqi Freedom* and *Operation Enduring Freedom* support this, as 53% of injuries sustained were penetrating soft tissue wounds and 26% were fractures [Owens et al. 2006]. Improvements in protective equipment and medical intervention have reduced the number of these injuries that ultimately prove to be fatal. However, this increase in survival rate has resulted in mounting concern for the rehabilitation of these soldiers.

The wounding mechanism of these injuries commonly results in extensive soft tissue damage that significantly impairs the function of the affected joint (Owens et al. 2006, Lin et al. 2004, Kjorstad et al. 2007). Soft tissue injury clinical complications may include wound infection, compartment syndrome, joint contracture and potentially amputation (Tu et al. 2008). If surgeons decide against amputation in favor of limb reconstruction, classic reconstruction techniques are currently used. These are limited to debridement, fracture fixation, soft-tissue management, and closure and skin grafting techniques (Javernick et al. 2006). These procedures do not restore any lost function to the area of injury but simply mend the injured area.

Advances in tissue engineering and stem cell research promise future treatments that may partially or completely regenerate lost muscle tissue and restore muscle function. Tissue engineering has entered clinical practice for a number of tissues, yet the field's application for the repair of muscle injuries sustained on the battlefield has not been studied. Surely, much work must still be done to fully realize the potential of these advances in a clinical setting.

The Regenerative Process: Skeletal Muscle

Repair of skeletal muscle under normal physiological conditions occurs in two distinct phases: a degenerative phase and a regenerative phase. The resulting inflammatory response acutely involves the activation of neutrophils, whose concentrations can remain elevated for days following injury (reviewed in Tidball 2005). These neutrophils can be phagocytotic or can release proteases that degrade cellular debris resulting from muscle damage. Their invasion into the tissue can also contribute damage the surrounding healthy tissue via direct lysis of muscle cell membranes through a superoxide-dependent mechanism, potentially causing defects in muscle contractility (Walden et al. 1990). Despite any additional damage, neutrophil-mediated debris removal is required for muscle repair as its inhibition is associated with slowed rates of muscle regeneration (Teixeira et al. 2003).

Following neutrophil invasion, macrophages are recruited to the injured area and contribute to the inflammatory process via phagocytosis and antigen presentation. These cells play a more intensive role in muscle repair and remodeling than simply clearing cellular debris. Remarkably, macrophages undergo a phenotypic switch to acquire an anti-inflammatory profile 24-48 hours after injury, once necrosis has slowed (Arnold et al. 2007). These converted macrophages proliferate and down-regulate the inflammatory response and stimulate myogenesis and fusion. Supporting data shows their *in vivo* depletion can decrease regenerating myofiber diameter or completely prevent muscle regeneration. Recent identification of growth factors derived from or controlled by macrophages, such as transforming growth factor-β (TGF-β) and heparin-binding EGF-like growth factor (HB-EFG), may partially explain these protective effects (reviewed in Tidball 2005). In this way, macrophages help transition to the regenerative phase of muscle repair.

After completion of the degenerative phase, the regenerative process closely resembles embryonic myogenesis. Commitment of cells to the myogenic lineage begins with the expression of Pax3 and results from signaling factors and cellular events of the surrounding tissues (reviewed in Wagers & Conboy 2005, Charge & Rudnicki 2004). Myogenic specification and cell expansion then requires the upregulation of myogenic regulatory factors (MRFs) at specific points during their development (reviewed in Sabourin & Rudnicki 2000). Included in these basic helix-loop-helix (bHLH) transcriptional factors are the "early" MRFs, MyoD and Myf5. Myoblasts can be defined as proliferative cells positive for these two markers. Their expression is required for the determination and propagation of skeletal myoblasts during embryonic development, as demonstrated by the complete absence of skeletal muscle in Myf5/MyoD double knockout mice (Rudnicki et al. 1993). Expression of the "late" MRFs, myogenin and MRF4, induce the terminal differentiation of myoblasts, withdrawing them from the cell cycle (reviewed in Hawke & Garry 2001). Finally, these mononucleated myoblasts then fuse with neighboring myofibers or with each other to form a multinucleated myocyte capable of developing into a contractile myofiber. These cells are also capable of migrating within the interstitial space between muscle fibers before their fusion and subsequent formation of small muscle fibers. Thought to play integral roles in these processes are M-cadherin, a transmembrane protein that mediates cell-cell interactions, and M-calpain, an intracellular nonlysosomal cysteine protease. Both are calcium-dependent and are preferentially expressed during this stage of regeneration (reviewed in Charge & Rudnicki 2004).

The regenerative process also heavily relies on the proliferation and migration of satellite cells to the site of injury. These cells reside within the basal lamina, juxtaposed between the plasma membrane and basement membrane of an individual myofiber (reviewed in Hawke & Garry 2001, Charge & Rudnicki 2004, Anderson et al. 2004). They do not differentiate into myocytes but are myogenic

progenitor cells that remain associated with a myofiber. Uniform expression of Pax7, a myogenic transcription factor, is required for satellite cell viability and can be used to identify these cells when coupled with the absence of MRF upregulation. Mitotically quiescent, these cells have a relatively small cytoplasmic area and reduced organelle content. Upon activation, they are capable of migrating within and between myofibers to contribute at the site of injury.

Several models for the postnatal renewal of the satellite pool have been proposed, and all may contribute to some degree as the clonogenic potential of this cell population is quite heterogeneous (Hawke & Garry 2001). Activated satellite cells may repopulate this pool through symmetrical satellite cell division, or symmetrical division followed by the withdrawal of some cells from the differentiation pathway to a state of quiescence (reviewed in Zammit & Beauchamp 2001). These ideas suggest that all satellite cells are capable of self-renewal. Alternatively, maintenance may be accomplished by a reserve compartment of resident and multipotent stem cells, aptly named muscle-derived stem cells (MDSCs).

Since their discovery, much research has focused on the role of MDSCs in skeletal muscle repair. Once activated, MDSCs are capable of differentiating along myogenic, osteogenic, chondrogenic and adipogenic lineages *in vitro* under the appropriate culture conditions (Asakura et al. 2001, Kuroda et al. 2006). These cells exhibit surface marker and gene expression of multiple mesenchymal lineages. Some evidence indicates an endothelial origin for these cells, as previous work has shown a cell population contained within skeletal muscle that coexpresses myogenic (CD56) and endothelial cell (CD34, CD144) surface markers (Tamaki et al. 2002, Zheng et al. 2007). However, this population is not well characterized and cellular origin has not been determined. Progenitor cells isolated from debrided, traumatized human muscle tissue possess the same differentiation potential of MDSCs (Nesti et al. 2008). Although they may originate in damaged tissue, it is

possible they have migrated to the site of injury from bone marrow, implicating the recruitment of nonmyogenic progenitor cells during skeletal muscle repair (Palermo et al. 2005).

Selecting a Stem Cell Population

Cellular therapeutics represents a vast range of these strategies and centers around stem cell research. A stem cell is defined as a clonogenic progenitor cell capable of both self-renewal and the generation of at least one differentiated cell type (Anderson et al. 2001). Indeed, muscle regeneration requires a cell population capable of sustained proliferation, self-renewal, multipotency and resistance to oxidative or hypoxic stress. While other considerations are certainly present and must be simultaneously addressed, the origin of those cells may largely determine the ability of that cell population to differentiate into the desired cell type and functionally contribute to an already-existing tissue or organ. Surely, selection of a cell population source and type is critical to optimizing treatment efficacy and avoiding associated complications.

First isolated from human embryos by Thomson et al. in 1998, embryonic stem (ES) cells have great developmental potential. Derived from the inner cell mass of the embryo and pluripotent in culture, ES cells can be induced to differentiate into all major cell types in the body and have a seemingly unlimited proliferative capacity. However, political and ethical concerns have currently disallowed federal funding of ES cell research in the United States. It was not until January 2009 that the FDA approved a human clinical trial using an ES cell-based therapy. Also, these cells by definition cannot be autologous and may elicit an immunogenic response. Induced pluripotent stem (iPS) cells, discovered in humans by Takahashi & Yamanaka in 2007, may be able to address these shortcomings. These cells can be generated from human somatic cells and genetically reprogrammed via retroviral transduction of specified transcription factors. However, while similar, these cells are not identical

to human ES cells and further studies are needed to determine whether iPS cells can replace ES cells in clinical applications. Until this can be accomplished, alternative sources of cells with similar capabilities must be heavily pursued.

Recently, adult stromal stem cells have generated a great deal of excitement in the scientific community. These undifferentiated cells reside in various tissues within the body and, much like ES cells, have an intrinsic ability to self-renew and differentiate into functional cell types when activated by mechanical cues within their local environment (Engler et al. 2004, Engler et al. 2006). Naturally responsible in part for the growth, maintenance, regeneration and repair of diseased or damaged tissue, these cells can be obtained directly from patients, eliminating the immune response associated with allogenic cells. Although not capable of generating cells characteristic of all three germ layers, these cells are multipotent and are capable of differentiation toward cell phenotypes unlike that of the tissue of origin. With the correct stimulus these cells can undergo transdifferentiation into a variety of cell types including osteocytes, adipocytes, chondrocytes, myocytes and neural tissue (Izadpanah et al. 2006, Zheng et al. 2006, Zuk et al. 2002).

MSCs, first discovered by Friedenstein et al. in 1970 and described as "adherent, spindle-shaped cells which proliferate to form colonies", are thought to give rise to cells of mesodermal lineage *in vivo*. Although these cells are not as accurately purified via stem cell marker identification as hematopoietic stem cells (HSCs), cell surface proteins Stro-1, SH2, SH3 and CD44 are helpful in creating a more homogeneous population of cells after extraction. Typically, MSC isolation relies on selective and spontaneous adherence to a solid surface while being grown in culture (Zheng et al. 2007). Cells isolated based on adherence are initially heterogeneous, containing a relatively high fraction of hematopoietic cells that are only lost after 2 to 3 weeks in culture (Prockop 1997). Because MSCs are isolated retrospectively in

culture, their *in vivo* microenvironment origin and identity are unknown. Despite being rare *in vivo* (roughly 1 in 100,000), a clinically relevant number of homogeneous cells can be attained following expansion in culture, making MSCs the cell population of choice for many researchers.

MSCs are most commonly derived from bone marrow, but recent interest in their derivation from adipose tissue has increased. BMSCs are advantageous simply because more literature has been published and we are more certain of their therapeutic effects during tissue regeneration. However, their extraction from the bone marrow is invasive, painful and therefore undesirable. Only a small sample of bone marrow can be extracted from a patient and the resultant cell population must be expanded in culture to attain a clinically relevant number of cells. Adipose tissue is easily obtained via liposuction. There is also the potential for point-of-patient care with adipose-derived stem cells (ADSCs) as a larger quantity and concentration of cells can be retrieved (Padoin et al. 2008), potentially large enough for immediate isolation and transplantation back into the damaged or diseased tissue. Some technologies claim to be able to perform this task, but the resultant cell population often is heterogeneous and may have effects deviating from a typically derived ADSC population. Nonetheless, ADSCs may prove to be an equally if not more efficacious stem cell population in some treatments.

Once in culture, cells from both populations behave in a similar manner, but not without differences worth mention. Human ADSCs are able to more quickly reach desired levels of confluency than human BMSCs (Izadpanah et al. 2006). ADSCs also seem capable of routinely expanding beyond passage 30 while human BMSCs began to senesce at passage 20. Although cells are rarely utilized during these late passages, this difference may indicate an inherent difference in population doubling potential and later impact their proliferative capacity *in vivo*. Population doubling times remained relatively consistent through passage 20 in ADSCs, while a

significant increase was seen in this same variable in BMSCs (Izadpanah et al. 2006). This loss is likely due in part to a decrease in telomerase activity with increasing passage number. Telomerase, an enzyme which adds a specific DNA sequence to the telomere of a chromosome following its division, gives the chromosome stability over time and is thought to play a large role in a stem cell's ability to self replicate. Morphological analysis reveals an increased cytoplasmic volume in later-passaged BMSCs, a characteristic not seen in ADSCs. Lee et al. support this data as their group also saw an increased proliferative capacity in ADSCs during later passages (Lee et al. 2004).

Cell surface marker expression as shown by immunofluorescence and flow cytometric analysis was consistent between both populations. Cells positively expressed Stro-1, SH2/SH3, CD29, CD44 and CD90, markers used to isolate stem cells and multilineage progenitors. These populations were also negative for HSC markers and others, such as CD13, CD31, CD34, CD45, at all passages (Izadpanah et al. 2006, Zuk et al. 2002). However, Zuk et al. identify two markers found to be unique, CD49d and CD106. CD49d, an alpha-4-integrin, is a known mediator of adhesive interactions between stem cell and stromal microenvironment. Its expression in ADSCs suggests these cells may be contained in a different microenvironment than BMSCs *in vivo*. CD106 promotes lymphocyte and monocyte adhesion and recruitment and is functionally associated with hematopoiesis and its expression in BMSCs correlates with their isolation from a tissue containing hematopoietic tissue. However, Izadpanah et al. saw expression of this marker in both cell populations; more work must be done to determine if this surface protein can accurately be used to differentiate between the two cell populations.

<u>The Role of Mesenchymal Stem Cells in Skeletal Muscle Repair</u>

MSCs are thought to be capable of differentiating into multiple lineages if induced to do so, and much literature is available on their ability to give rise to osteocytes,

adipocytes and chondrocytes *in vitro* (Pittenger et al. 1999, Zuk et al. 2002, Baksh et al. 2004). BMSCs, characterized by many of the same cell surface markers discussed previously, indeed show tri-lineage potency, indicating that they are in fact stem cells as opposed to a collection of multiple lineage-specific precursors (Pittenger et al. 1999). Using a very homogeneous and reproducible cell population isolated using the adherent cell technique, cultured cells presented with lineage-specific induction mediums expressed adipogenic, osteogenic and chondrogenic markers while simultaneously undergoing morphological changes typical of that cell type. Furthermore, the presence of lineage-specific markers demonstrating functional maturation can be maintained in culture.

ADSCs can also differentiate *in vitro* towards mesodermal lineages, including osteogenic, chondrogenic and adipogenic lineages following treatment with lineage-specific differentiation factors (Zuk et al. 2002). However, despite displaying this same multilineage potential, these cells form a more heterogeneous population containing endothelial cells, pericytes and smooth muscle cells (Zuk et al. 2001). These cells display their differentiation capabilities through 2-4 weeks of induction in lineage-specific differentiation mediums, expressing phenotypic and genetic profiles consistent with those seen in other studies and in mature adipocytes, chondrocytes and osteocytes (Zuk et al. 2002). A direct comparison between these two cell populations reveals a similar phenotypic expression of markers specific to adipogenic, chondrogenic and osteogenic lineages through passage ten, past what many investigators believe to be an acceptable cell life for use in therapeutic applications (Izadpanah et al. 2006). However, not all cells in culture expressed these changes, having a more restricted dual or single lineage potential. As little as 35-40% of cells in some cultures exhibit a morphology consistent with their intended phenotype in both populations. Because this potential was lost after some time, it is unclear as to whether these cells would maintain their expression patterns following *in vivo* implantation.

MSCs have also been implicated with myogenic differentiation *in vitro*. A novel strategy for inducing this differentiation in rat and human BMSCs was presented by Dezawa et al. in 2005. Briefly, adherent MSCs negative for c-kit, CD34 and CD45 were expanded through passage 3 and then treated with a myogenic induction medium. The Notch signaling pathway was then activated via intracellular gene transfer; this pathway has been shown to control the functional development and stabilize phenotype during several cell differentiation processes. Finally cells were treated with a fusion medium to induce the formation of multi-nucleated myotubes. Following 10 days in this medium 40% of cells spontaneously fused. These cells also displayed morphological and phenotypic changes consistent with mature myotubes both *in vitro* and *in vivo*. Expression of MyoD, an early protein marker of myogenic differentiation, myosin heavy chain (MHC), a motor protein associated with mature myofibers, and Pax-7, a satellite cell marker, were observed in all cell populations via immunofluorescence, Western blotting and reverse transcription polymerase chain reaction (RT-PCR, Dezawa et al. 2005).

This myogenic potential is not unique to BMSCs, as ADSCs also demonstrated expression of MyoD and MHC following induction in a myogenic medium via immunofluorescence and RT-PCR (Mizuno et al. 2002). Spontaneous cell fusion was also seen in these myogenically induced cells three weeks post-induction. However, this study did not characterize these cells before myogenic induction and it is unknown as to whether other cells present in a previously found heterogeneous population may have contributed to these findings. Zheng et al. showed ADSCs possess a limited ability to undergo myogenic & hematopoietic differentiation but a high capacity for osteogenic & chondrogenic differentiation. Different anatomical locations of adipose tissue may have different gene expression profiles, and attachment & proliferative capacity are more pronounced in ADSCs from younger donors (Zheng et al. 2006).

Cells derived from bone marrow may be able to incorporate themselves into existing skeletal muscle under certain conditions (Grounds et al. 2002). Following myogenic induction and myotube formation, human bone marrow-derived stem cells (BMSCs) are able to engraft into muscles damaged with a cardiotoxin following local or intravenous injection into mdx-nude rats (Dezawa et al. 2005). BMSCs tagged with green fluorescent protein (GFP) stained positively for myogenic markers and *in vivo*, while Pax-7-positive BMSCs were seemingly incorporated into the satellite cell population. Perhaps most impressively, transplanted myofibers containing only a few satellite cells were capable of repopulating the satellite cell pool in irradiation-depleted muscle and giving rise to new myofibers within the damaged muscle (Collins et al. 2005). These results persisted for at least eight weeks as satellite cells remained capable of activation and repair, even in response to injury. Therefore, at least a portion of these Pax7(+) cells are, by definition, stem cells, as they exhibit an ability to self-renew and generate a functional tissue type.

BMSC contribution in response to physiological stressors was demonstrated in a surgical parabiosis model enabling GFP-labeled circulatory cells from transgenic animals to access wildtype tissues via blood chimerism (Palermo et al. in 2004). Cell engraftment derived from bone marrow and transported to the affected tissue via circulation was evident in response to cardiotoxin treatment, forced eccentric exercise and muscle overload models. While these results are promising, it is difficult to quantitatively assess the level of engraftment as data was obtained from muscle cross sections. Multinucleated myofibers will likely express GFP, a diffusible cytoplasmic protein, if only one GFP-positive BMSC is incorporated into the tissue. Nevertheless, cellular engraftment does occur under normal physiological stressors and strongly indicates a role in non-muscle cells to follow the myogenic lineage and contribute to skeletal muscle repair.

Skeletal Muscle-Derived Extracellular Matrix as a Biologic Scaffolding

Skeletal muscle tissue can be decellularized such that all that remains is a biologic scaffold (Badylak 2007). This extracellular matrix (ECM) is primarily composed of collagen and void of all cellular material and soluble proteins, rendering it nonimmunogenic (Borschel et al. 2004, Ott et al. 2008). Its three-dimensional geometry allows for the transduction of mechanical force throughout the construct. The decellularized ECM has been shown to be capable of supporting and guiding myofiber ingrowth (Borschel et al. 2004, Merritt et al. 2009) and retains the specific and complex infrastructure necessary for recellularization of vascular bed and peripheral nervous system (Kochupura et al. 2005). Proper substrate compliance dictates the mechanical signaling necessary to drive the differentiation and striation of regenerated myotubes, characteristics inherent of ECM derived from skeletal muscle tissue (Engler et al. 2004, Engler et al. 2006). However, implantation of the ECM itself does not restore function (Merritt et al. 2009) and cellular repopulation has been shown to substantially improve overall function (Kochupura et al. 2005).

Reinnervation & Vascularization of a Skeletal Muscle Construct

Both the revascularization and reinnervation of a muscle construct is required for complete and sustained recovery of tissue function. Failing to supply and exchange oxygen and nutrients will likely result in the formation of a hypoxic region unable to support myofiber growth, while a denervated fiber will not fully mature or contribute to a muscle's functional output. In healthy skeletal muscle, a breakdown in the microvascular blood supply will cause progressive myonecrosis (Charge & Rudnicki 2004). The innervation of a newly formed myofiber allows for the expression of characteristic physiological properties seen in a mature myofiber, including specific MHC isoforms and various metabolic enzymes. Surely, these two objectives must be accomplished to fully restore and maintain function in a developing construct.

There are two sources of denervated fibers following injury: a regenerating myofiber and the distal portion of a transected myofiber. Failure to innervate a regenerating myofiber will prevent full maturation, while denervation of a previously healthy myofiber will likely induce muscle atrophy, fibrosis and irreversible changes in the properties of the muscle membrane. In the later, resident satellite cells are activated immediately following damage and may remain active for several weeks due to their denervated state, as evidenced by the labeling of activated satellite cells using neural cell adhesion molecule (NCAM, Borisov et al. 2005). Their proliferation and fusion with parent myofibers may slow this process initially, but following long periods of denervation the satellite cell pool is exhausted. This signifies a progressive decline in the muscle's intrinsic regenerative capacity following long-term denervation (Borisov et al. 2001, Borisov et al. 2005). Conversely, an increased density of satellite cells has been observed at motor neuron junctions and adjacent to capillaries (Borisov et al. 2001). This evidence directly links regenerative capacity as measured by satellite cell count to these structures while also suggesting they emit factors that play a role in the distribution and regulation of the satellite cell pool.

A strong link exists between vascular maintenance and development and the regenerative capacity seen in denervated muscle. A well-vascularized construct has also been shown to enhance nerve regeneration (Hobson et al. 1997), while prolonged denervation stimulates the degeneration of the associated vasculature (Borisov et al. 2001). The resulting avascular areas within muscle likely contribute to the irreversibility of the regenerative process. Moreover, continued regeneration and terminal differentiation of neomyofibers is likely prevented when contained within an avascular, and therefore hypoxic, area (Li et al. 2007). Supporting data demonstrates the migration of satellite cells following denervation occurs in the direction of capillaries, indicating the differentiation of new muscle fibers may require oxygenation (Borisov et al. 2005). Indeed, satellite cells cultured at low

(<2%) levels of oxygen see inhibited myogenic differentiation (Di Carlo et al. 2004). This is not to say that excess oxygen is beneficial, however; the atmospheric concentration of oxygen is not as effective as those levels that exist in skeletal muscle (3-6%). Cells cultured in these conditions see an increase in developmental potential, proliferative capacity and an accelerated up-regulation of myogenic regulatory factors (Chakravarthy et al. 2001, Csete et al. 2001). Clearly, connection to the vascular system for efficient transport of oxygen, carbon dioxide, nutrients and waste products is vital to the development of both myofibers and nervous tissues following injury.

Transplantation of MDSCs into severely damaged skeletal muscle resulted in a significant increase in mass and functional recovery, as well as their contribution to the growth of myofibers, blood vessels and nerve fibers within the damaged area as detected by GFP labeling of transplanted MDSCs (Tamaki et al. 2005). Their contribution to vascular and neural tissues *in vivo* can likely be attributed, in part, to their differentiation into endothelial and Schwann cells (Qu-Petersen et al. 2002). Contributions to these newly developed structures were not entirely made by transplanted MDSCs, however, suggesting the existence of tissue-specific or circulating progenitor cells in the process.

SIGNIFICANCE OF STUDY

The knowledge gained pertaining to muscular regeneration will directly benefit combat soldiers in our military. Doing all that we can to restore of the physical abilities lost subsequent to injury sustained in combat is a moral obligation we have to our soldiers. Practically, the restoration of function to these soldiers will be of great help to maintaining our combat forces. There are also financial benefits from this research, as a large sum of money has been invested to train these soldiers. Furthermore, their functional restoration will greatly reduce long-term rehabilitation costs. From a more general view, it is beneficial to them and our society to have these men and women functioning as active and independent members of society.

The basic science developed in this research will benefit the medical community in restoring skeletal muscle function to its patients. Those who have been injured in civilian-related trauma and in diseased states resulting in muscular degeneration, such as muscular dystrophy, can benefit greatly. Moreover, this research will make contributions to the literature concerning the role of bone marrow-derived stem cells, adipose-derived stem cells and the nerve relocation procedure in skeletal muscle repair and regeneration. A direct comparison between the two cell populations regarding their impact on functional recovery following tissue loss has not been made up to this point and the knowledge gained on this subject will be welcomed in the scientific community. Finally, this research should lead to further studies concerning the growth, development, innervation and revascularization of regenerated skeletal muscle and the factors that contribute to this process.

METHODS

Male Lewis rats (Charles River Laboratories; Wilmington, MA) 6-9 months of age were used in this study. Rats were housed individually, maintained on a 12-hour light/dark cycle and allowed *ad libitum* access to food and water. Rats were randomly assigned to experimental groups and were evaluated functionally and histologically following 42 days recovery (n = 6-8). All animals were obtained from the Animal Resource Center at the University of Texas at Austin and treated in compliance with the ethical guidelines of the Institutional Animal Care and Use Committee (IACUC).

Cell Culture

Adipose-Derived Stem Cells: Adipose tissue was obtained from rat lipoaspirates and cultured as described by Zuk et al. in 2001. To isolate the stromal vascular fraction (SVF), raw lipoaspirate was washed extensively with equal volumes of phosphate buffered saline (PBS). Washed aspirates were treated with 0.075% collagenase in PBS for 30 minutes at 37°C. Enzyme activity was neutralized with Dulbecco's modified Eagle's medium (DMEM) containing 10% fetal bovine serum (FBS) and 1% antiobiotic/antimycotic (AA) solution. High-density SVF pellets were obtained by centrifugation at 1200g for 10 min and resuspended in 160 mM ammonium chloride for 10 minutes at room temperature to lyse contaminating red blood cells. Centrifugation was repeated (1200g for 10 min) and SVF pellets were filtered through 100-μm nylon mesh to remove cellular debris. The filtrate was plated on conventional tissue culture plates in a non-inductive control medium containing Dulbecco's modified eagles medium (DMEM), 10% fetal bovine serum (FBS) and 1% AA solution and incubated overnight at 37°C and 5% CO_2. Plates were washed extensively with PBS to remove residual non-adherent cells. The resultant adherent fraction was maintained at 37°C and 5% CO_2 and passaged as the cells reached 70% confluency.

Bone Marrow-Derived Stem Cells: Bone marrow was obtained from the surgically removed femur and tibia of Lewis rats by flushing the shaft with media using a 10 mL 18G syringe. Cells were disaggregated by gently pipetting and centrifuged at 1000g for 5 min at 4°C. The resulting pellet was resuspended in media, plated on conventional tissue culture plates in the same non-inductive control medium used for ADSCs and incubated overnight at 37°C and 5% CO_2. The resultant adherent fraction was rinsed and maintained at 37°C and 5% CO_2 and passaged as the cells reached 70% confluency.

Extracellular Matrix Preparation

The skeletal muscle-derived extracellular matrix (ECM) was prepared from GAS removed from a separate group of male Lewis rats and decellularized using a method similar to Borschel et al. (2004). Upon extraction, muscles were place in deionized water at 4°C for 24 hours to cause swelling and membrane rupture. Muscles were then placed in chloroform for 72 hours, followed by continuous agitation within 2% sodium dodecyl sulfate (SDS). The 2% SDS solution was changed twice per week until all cellular components were removed, leaving only the collagenous interstitial matrix. The remaining ECM was rinsed in deionized water with 3 solution changes per day over 48 hours to rid the ECM of SDS. ECMs were then rinsed for 4 hours in a 0.1 M tris buffer solution (TBS, pH = 9.0). Finally, the ECM was submerged in phosphate buffered saline (PBS) with 1% penicillin/streptomycin (Sigma-Aldrich; St. Louis, MO), exposed to UV light for ≥12 hours and stored at 4°C until its implantation into the defect area.

Surgical Procedures

Prior to surgery, animals were randomly placed in one of six experimental groups: implantation of the ECM (MAT), implantation of the ECM followed by ADSC injection (AD), implantation of the ECM followed by BMSC injection (BM), implantation of the

ECM followed by redirection of the peroneal nerve (N), implantation of the ECM followed by peroneal nerve redirection and ADSC injection (AD+N) and implantation of the ECM followed by peroneal nerve redirection and BMSC injection (BM+N). All surgery was performed under aseptic conditions and with sodium pentobarbital (65 mg/kg body weight) anesthesia via intraperitoneal injection.

All animals underwent surgery to remove a portion of the lateral gastrocnemius (LGAS) and replace the lost tissue with a homologous ECM (Figure 1B). A ~2.0 cm incision was made into the skin at the lateral side of the lower leg parallel to the tibia. The biceps femoris was separated from the tibia to expose the lateral portion of the LGAS. Following isolation from the soleus, a 1.0 x 1.0 cm portion of muscle was excised from the LGAS and the mass of the defect was recorded. The injury was repaired by the implantation of the ECM immediately followed the removal of the defect, aligned in parallel with the transected myofibers. Using a non-absorbable polypropylene 5-0 suture, a modified Kessler stitch with simple interrupted sutures on all 3 borders was utilized to secure the ECM into the defect area and serve as markers for later analysis (Kragh et al. 2005).

MSC Injection: Following a 7-day recovery period to avoid the inflammatory response resulting from the initial injury, the LGAS was exposed using previously described methods. Approximately 1.5×10^6 MSCs, suspended in 2.0 mL PBS and harvested between passages 3 – 8, were injected at several points into the ECM (Figure 1C). The injury was then repaired using the same methods as described above.

Nerve Redirection: The LGAS was exposed using previously described methods. A ~1.0 cm incision was made into the skin at the medial side of the lower leg parallel to the tibia. The peroneal nerve was denervated as distally as possible and redirected through the anterior and posterior compartments to the defected area

(Figure 1D). Oriented within the defected area and perpendicular to myofibers of the LGAS, the nerve was secured to the ECM with one non-absorbable polypropylene 5-0 suture. The biceps femoris was then reattached to the tibia and both incisions to the skin were closed using a non-absorbable polypropylene 5-0 suture.

Functional Analysis

Following the recovery period, *in situ* measurements were performed on both the experimental leg and the contralateral (internal control) leg. To functionally isolate the LGAS, the branch of tibial nerve was severed from the medial head of the gastrocnemius and the distal portion of the gastrocnemius was separated from the plantaris and soleus. The calcaneus was detached and the Achilles tendon attached to a servomotor muscle lever system (Aurora Scientific). The sciatic nerve was stimulated to elicit a maximal isometric tetanic contraction. The muscle was kept wet in mineral oil and the temperature was maintained between 36.5°C and 37.5°C with a radiant heat lamp. The muscle length was adjusted to optimal muscle length with a micrometer, while maximal twitch tension was determined using stimulation at 0.5 Hz and 7 V. For peak tetanic tension, the muscle was stimulated at 150 Hz and the minimum voltage necessary to elicit maximal contraction. After each contraction, the muscle was allowed to rest for 2 minutes. Total force and specific tension were determined.

Histological Analysis

Following functional analysis, the experimental LGAS was excised, cleaned of excess fat and external connective tissue, weighed and frozen in isobutane at -150°C, cooled in liquid nitrogen. Series of 5 μm sections perpendicular to myofiber orientation and within the distal, central and proximal regions of the implanted ECM were made using a Leica CM1900 cryostat microtome (Leica Microsystems; Wetzlar, Germany) at -20°C and allowed to dry overnight at room temperature. To identify

regions of cellular material and collagen-containing ECM, Masson's trichrome (Sigma-Aldrich; St. Louis, MO) staining was performed. A rabbit anti-human polyclonal antibody against von Willebrand factor (vWF, 1:300: Dako; Carpinteria, CA) was used to identify blood vessels, as this glycoprotein is present in platelets as well as endothelial cells of the vessel wall. The signal was enhanced with biotinylated polyclonal goat-anti-rabbit IgG with streptavidin-HRP. Color was developed after incubation with 3,3-diaminobenzidine (DAB).

In preparation for immunofluorescent identification, sections were permeabilized with 2N HCl, washed in tris-buffered solution containing 0.5% Tween 20 (TBST) and blocked with 10% normal donkey serum in TBS containing 1% bovine serum albumin (BSA). All of the following materials were purchased from Santa Cruz Biotechnologies, Santa Cruz, CA unless otherwise stated. Sections were first incubated with primary antibodies against the cytoskeletal protein desmin (1:400, goat polyclonal) or the striated muscle-specific motor protein myosin heavy chain Y-20 (MHC, 1:400, goat polyclonal) and detected with a donkey anti-goat IgG-FITC fluorescein (1:100, λ = 495 nm). Sections were then incubated with a primary antibody against structural glycoprotein laminin β-1 (1:400, mouse monoclonal) and detected with a donkey anti-mouse IgG-TRITC fluorescein (1:100, λ = 546 nm). Finally, sections were counterstained with Hoescht 33258 (1:1000, λ = 395 nm: AnaSpec; San Jose, CA) to identify nuclei. Subsequent to a final series of washes in TBS, sections were mounted in Permount mounting medium (Fisher Scientific; Waltham, MA).

Imaging & Analysis: Masson's trichrome- and vWF-stained sections were visualized with a Nikon Diaphot microscope mounted with an Optronix Microfire digital camera. Immunofluorescence was visualized with a Leica DM LB2 fluorescence microscope and photographed with a Leica DFC340FX digital camera *(*Leica Microsystems; Wetzlar, Germany). Histological quantification of Masson's

trichrome and vWF was performed on each level and within the region of the ECM (n = 3). In each group, 3 images were taken at 200x magnification and analyzed. Cellular content within each region of the ECM implant was quantified using LabView and expressed as a percentage of the total image area. The number of vWF-positive structures within each region of the ECM implant was counted to determine the number of blood vessels/mm^2. A vessel was only counted if its lumen was greater than 20 μm in diameter. Counts were performed by investigators who were blinded to the treatment.

Statistical Analysis

Data are represented as mean ± SEM. Statistical analysis was performed utilizing three-way ANOVA for analysis of group samples. Comparisons between data sets were performed utilizing unpaired *a priori* student's t-tests and Tukey's post hoc tests where available. Statistical significance is defined as $p < 0.05$.

RESULTS

Morphological Analysis

The average mass of the muscle defect removed from Lewis rats was 181 ± 3 mg wet muscle weight, accounting for approximately 15% of the total mass of the LGAS. No significant differences in defect mass existed between groups or within groups. Thus, a significant portion of the tissue was removed, providing sufficient area for myofiber regeneration and ingrowth to be studied.

Consistent with previous work by Merritt et al., overall morphology of the LGAS was visually maintained following ECM implantation in all animals (Merritt et al. 2009). This is supported by a nearly complete restoration in the mass of the injured LGAS, which was 97.9 ± 1.0% of the mass of the contralateral LGAS. No significant differences existed between these groups. Also, no significant differences in the injured LGAS mass following the 42-day recovery period existed between groups or within groups.

Functional Analysis

Following 42 days recovery, implantation of the ECM with no further treatment resulted in functional impairment of the LGAS. Maximal isometric tetanic force (P_O) produced in the MAT group was 85.1 ± 4.1% of that produced in the contralateral LGAS. No significant differences were seen in P_O produced by the injured LGAS between the MAT group and all other groups (Figure 2). However, BM and BM+N treatments did increase this measure significantly by 15.3% and 18.7% over the AD treatment, respectively.

Functional performance was also expressed using specific tension (SPo), the maximal isometric tetanic force normalized to LGAS cross sectional area. A significant increase in SPo was seen in all groups that underwent the nerve

relocation procedure, rising 11.0%, 14.3% and 11.5% in the N, BM+N and AD+N groups when compared to the MAT group (Figure 2). When directly stimulating the redirected peroneal nerve, however, no contraction was visualized or measureable force produced. The BM group displayed a trend towards significance when compared to the MAT group ($p = 0.059$). Conversely, AD group values for both MF and SPo (82.6 ± 2.8%) were reduced below the MAT group. Although not significantly different, these data suggest an inability of those cells to stimulate recovery in a way that would contribute to our measure of force production.

Histological Analysis

Histological analysis of the defect area following 42 days of recovery confirms the presence of regenerating myofibers and blood vessels within the ECM. Quantification of cellular content in normal, healthy muscle tissue via Masson's trichrome staining demonstrated a dense packing of myofibers, accounting for 97.6 ± 0.5% of the total image area ($n = 12$). Cellular content was significantly lower in all study groups and regions when compared to healthy tissue (Figure 4). In all groups, the area closest to the implantation border (as identified by suture holes) appears to be most densely populated, with fewer myofibers seen further into the ECM.

Regenerating myofibers contained by the ECM following BMSC injection occupied a significantly greater area than those without BMSCs. Cellular content in the top and bottom groups increased significantly by 253.8% and 61.3% in the BM group and 187.6% and 57.1% in the BM+N group over the MAT group, respectively (Figure 3A). However, BMSC injection did not make a significant contribution to cellular content in the middle region of the ECM. Consistent with functional analyses, the AD group did not see an improvement in cellular content in any region when compared to the MAT group. In fact, these values were significantly lower when compared to the BM group. These same results are seen when measuring blood vessel density

within the ECM via staining for vWF. Blood vessel density (per mm^2) significantly increased by 73.1% and 111.1% in the top and bottom regions of the BM group when compared to the MAT group (Figure 3B). In the BM+N group, a significant increase of 50.0% was seen in the bottom region but not the top, an insignificant increase of 23.1%. AD group values were not significantly different to MAT values and significantly lower than BM values.

Interestingly, all groups that did receive the nerve relocation saw a significant increase in the cellular content of the middle region when compared to all groups lacking this treatment (Figure 5). N, BM+N and AD+N groups were all significantly higher than MAT, BM and AD groups by 172.7%, 37.5% and 211.1%, respectively (Figure 3A). When inspecting blood vessel density data, a similar result occurred (Figure 6). Following nerve relocation, blood vessels per mm^2 in the middle region of each group were significantly higher than the corresponding value in groups that did not receive the nerve relocation treatment (Figure 3B). Both cellular content and blood vessel density in the middle region of all nerve relocation groups were not significantly different from both the top and bottom regions. This difference was statistically significant for both variables in the BM group.

Finally, the presence of regenerating myofibers as originally identified with Masson's trichrome staining was further confirmed by immunohistochemical analysis. Colocalization of desmin or myosin heavy chain (MHC) with laminin was observed in structures contained within the ECM (Figure 7). The presence of central nuclei, identified by Hoechst 33258, substantiate their identify as regenerating myofibers.

DISCUSSION

As shown previously, removal of the defect and subsequent implantation of the ECM results in sustained functional damage that does not repair itself following 42 days recovery (Merritt et al. 2009). This is partially due to the complete loss of cellular material within the implanted ECM. Much literature exists endorsing BMSCs as capable of myogenic differentiation and contribution to muscle regeneration *in vivo* (Ferrari et al. 1998, Dezawa et al. 2005). This study is in agreement with these researchers, showing that injection of BMSCs into the implanted ECM results in an improved functional output and increased cellular content. These regenerating myofibers often possessed central nuclei and exhibited a colocalization of desmin and myosin heavy chain with laminin, indicative of differentiating myofibers. Increases in cellular content primarily occurred in the top and bottom regions adjacent to transected myofibers, suggesting the ingrowth of injured myofibers from the superior and inferior portions of muscle remaining after the defect injury as the most likely method of functional improvement. Although not determined in this study, conflict exists as to the specific role of BMSCs during skeletal muscle repair. Differentiation into myofibers or fusion with existing myofibers may play a role in these improvements. However, cellular engraftment appears to be a relatively rare event, reported to occur in 3-12% of regenerating myofibers (Palermo et al. 2005, Dezawa et al. 2005). Coupled with other reports of improved muscle function without evidence of myogenic differentiation or fusion of injected cells (reviewed in Prockop 2009), it seems likely that other mechanisms contribute to functional repair.

The development of a functional skeletal muscle construct must not only concern the myofiber ingrowth, but also the formation of a vascular framework within the construct capable of supporting the regenerating musculature. Not surprisingly, in all regions and treatments, areas of increased cellular content within the implanted

ECM coincided with an increased blood vessel density. BMSC injection resulted in a significant increase in blood vessel density in the top and bottom regions of the ECM. Again, although capable of differentiating into endothelial cells, cellular incorporation of BMSCs is rare, occurring in between 5 and 26% of newly formed vessels (Murayama et al. 2002). In response to low cellular engraftment of BMSCs in both tissues, we highlight their ability to produce related trophic factors able to aid the vascularization of injured muscle. BMSCs have been shown to participate in autocrine/paracrine signaling mechanisms that stimulate or directly cause the release of growth factors, cytokines and chemokines (Prockop 2009). In fact, it is the ability of BMSCs to produce vascular endothelial growth factor (VEGF) that likely contributes to neoangiogenesis *in vivo* (Al-Khaldi et al. 2003). Surely, cellular tracking within our model is needed to determine the extent of cellular incorporation into myofibers and vascular structures as a means of improving functional output.

When selecting a stem cell population, one must not only consider its regenerative potential, but also its relevance to a clinical setting. Both the ease and efficiency of surgical procurement as well as increased potential for point-of-care preparation of the cell concentrate make ADSCs an attractive alternative to BMSCs. However, as stated earlier, the data presented here demonstrate an inability of ADSCs to improve functional recovery of a skeletal muscle defect repaired with an implanted ECM. Furthermore, ADSC injection did not result in an increased cellular content or blood vessel density when compared to its control. ADSCs can be myogenically induced *in vitro* (Mizuno et al. 2002) and seem capable of efficacious utilization. However, expression of markers characteristic of another cell type does not necessarily result in a functioning cell type under normal physiological conditions *in vivo*. Removal from their stromal microenvironment may induce differentiation and alter phenotypic expression patterns, while their implantation may alter those expression patterns induced *in vitro*. Certainly, ADSCs must demonstrate more

robust and persistent regenerative potential in a target environment to warrant continued study within this model.

While BMSC injection was shown capable of improving cellular content in the top and bottom regions of the ECM implant, the middle region remained relatively acellular. Should BMSCs aid the regenerative process largely by stimulating the release of growth factors and not via engraftment, their effects may not endure enough to positively impact this diffusionally limited region. The lasting relocation of the peroneal nerve did restore a significant amount of cellular material to the middle region and can be attributed, in part, to the previously discussed neurotrophin release associated with the transplanted nervous tissue (Lavasani et al. 2006, Deponti et al. 2009). Still, some degree of innervation is implied by significant improvement in functional output without a significant increase in cellular content in the top and bottom regions. Surely, this invalidates the enhanced ingrowth of injured myofibers as a potential mechanism. However, neurotization resulting from this procedure seemingly did not occur as no measureable force was produced following direct electrical stimulation of the peroneal nerve.

Direct contact of the relocated peroneal nerve with a viable motor endplate can lead to successful reinnervation of a denervated or regenerating myofiber (Bixby & Van Essen 1979). The middle region of the ECM contains only regenerating myofibers and any existing motor endplates present on these myofibers must form ectopically during regeneration. This event is a desired but unlikely contributor to regenerating myofiber innervation when both the extent of injury and the spatial and temporal concerns of our model are considered. Moreover, the presence of a viable endplate is not necessary for the formation of a neuromuscular junction (NMJ) during development. Contact between a denervated myofiber and the motor axon terminal stimulates the secretion of agrin. Activated agrin receptors, in combination with a muscle-specific kinase MuSK, are known to promote a clustering

of acetylcholine receptors (AChRs) in the postsynaptic membrane (Valenzuela et al. 1995, Strochlic et al. 2005). Neural growth factor (NGF) has been shown to enhance ectopic NMJ formation in denervated myofibers (Iwata et al. 2006) and may aid the formation of regenerating myofibers in this model. Certainly, NMJ formation in this manner is a potentially limiting factor to the innervation of myofibers within the ECM and must be addressed in future studies.

The use of electrical stimulation prior to innervation in this model may help to develop and sustain ectopic endplates and NMJs. It has been shown to increase AChR clustering while decreasing the level of AchR diffusion and subsequent degradation of neuromuscular junctions following the denervation of skeletal muscle (Kang et al. 2003). While it can prevent the innervation of a denervated myofiber by a foreign nerve, be it from its original innervation or elsewhere, electrical stimulation does not prevent the growth of nerve fibers in the area (Jansen et al. 1973). If utilized at the correct times during development, electrical stimulation may benefit this process and should be considered as a treatment option.

Initially, myofiber regeneration within the middle region is promising but must be supported by associated vasculature. The center of the ECM without vasculature, due to diffusive capabilities of oxygen, is assumed to be largely hypoxic. Interestingly, neurotrophic factors, in parallel with their neuroprotective and myogenic effects discussed previously, organize neoangiogenesis to support the innervation and blood supply in ischemic areas (Kermani et al. 2005). Tyrosine kinase (Trk) receptors have been shown to exist in human and rat vascular smooth muscle cells (Donovan et al. 1995). Endogenous NGF expression increases in response to local ischemia, and daily injections of NGF has been shown to markedly increase arteriole length density in ischemic muscle (Turrini et al. 2002). Exogenous delivery of NGF participates in reparative capillary formation, triggered

by ischemic conditions (Emanueli et al. 2002). NGF may act through the stimulation of other angiogenic factors such as VEGF, rather than directly activating vascular growth. Brain-derived neurotrophic factor (BDNF), known to support long-lasting augmentation in vessel integrity and stability, also supports neoangiogenesis *in vivo* (Kermani et al. 2005). These effects are comparable to that of VEGF and occur through the recruitment of endothelial cells, including bone marrow progenitor cells, expressing the TrkB receptor in skeletal muscle.

This work demonstrates the efficacy of BMSC injection and peroneal nerve relocation to the regeneration of a functional skeletal muscle construct contained by an implanted ECM *in vivo*. These treatments may work through direct cellular contribution or the release of trophic factors to stimulate myogenesis and angiogenesis. The performance of additional studies concerning the identification and actions of neurotrophins and angiogenic factors within the ECM, will substantially enhance our understanding of the mechanisms underlying skeletal muscle regeneration. Also, efforts must be made to reconstitute nervous tissue within a construct, as it is vital to functional recovery and may be essential to the terminal differentiation, maturation and long-term sustenance of regenerated tissues. In doing so, this work may lead to the development of clinically relevant therapies aimed at the treatment of wounded military soldiers suffering from skeletal muscle tissue loss.

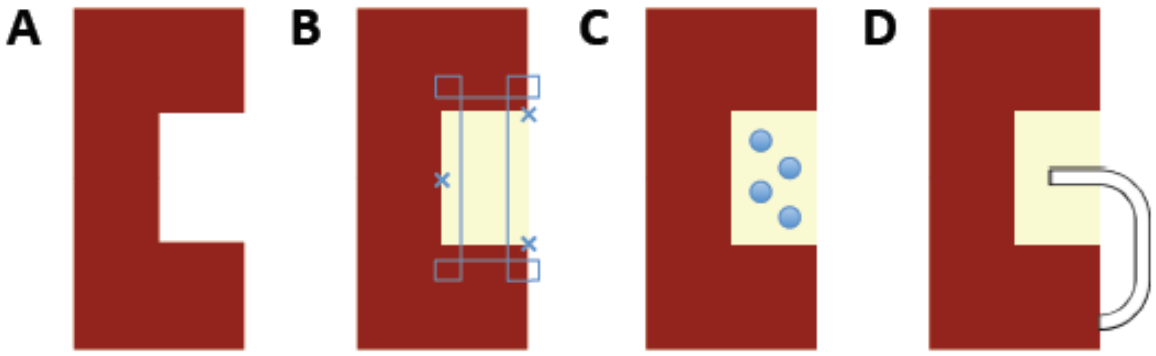

Figure 1: Schema of surgical procedures performed. [A] Defect removal. [B] ECM implantation. [C] MSC injection. [D] Nerve relocation. Blue lines represent sutures, blue circles represent MSCs, white arrow represents the relocated peroneal nerve.

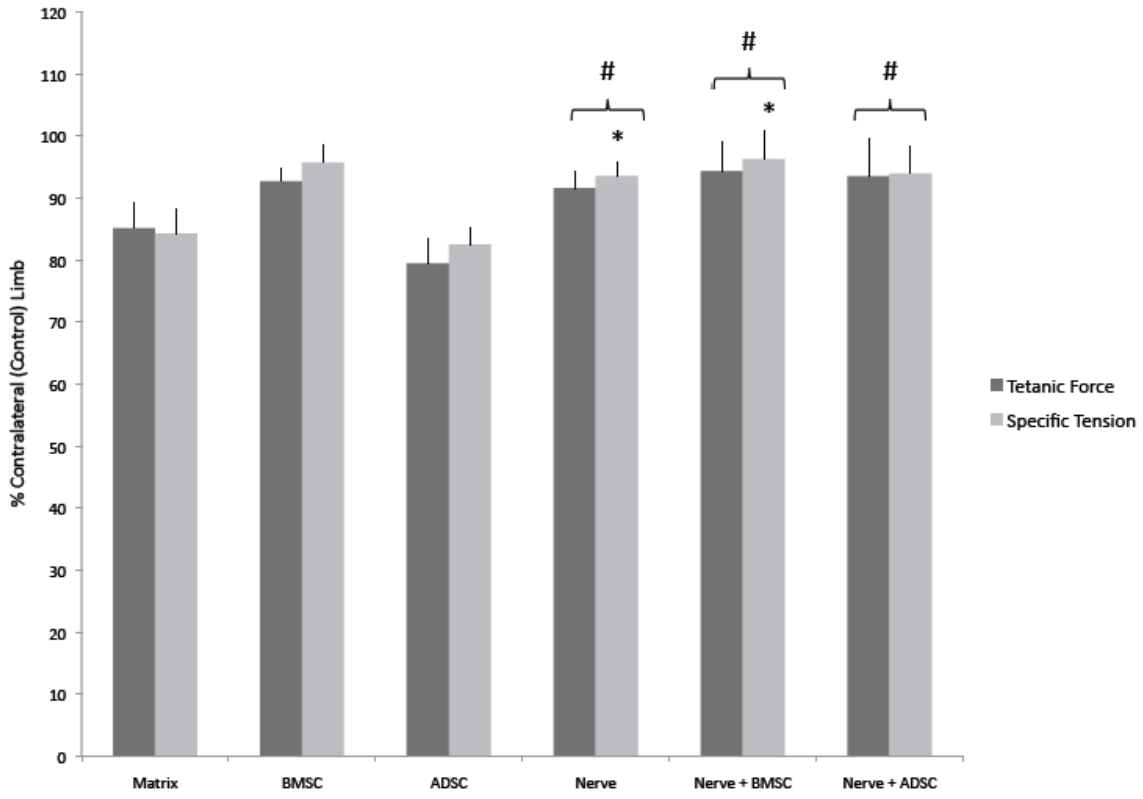

Figure 2: Force production (N) and specific tension (N/cm^2) resulting from maximal isometric tetanic contraction of the LGAS containing the defect. Following 42 days recovery. Relative to the contralateral limb. * Indicates statistical significance from MAT group ($p<0.05$). # Indicates statistical significance from ADSC group ($p<0.05$).

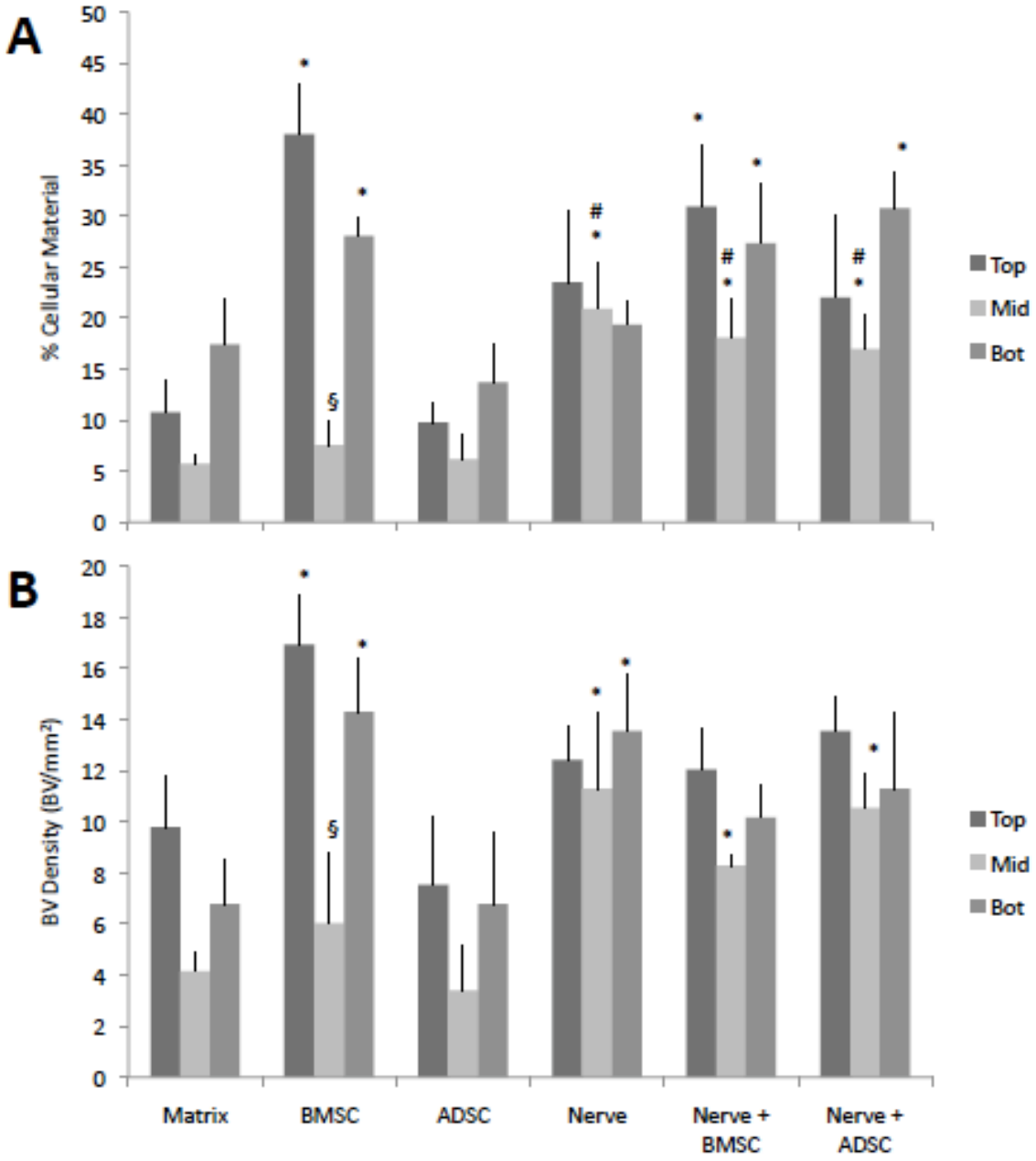

Figure 3: Histological quantification of [A] cellular content and [B] blood vessel density within the top, middle & bottom regions of the defect following 42 days recovery. * Indicates statistical significance from MAT group ($p<0.05$). # Indicates statistical significance from all groups not involving nerve relocation ($p<0.05$). § Indicates statistical significance from the top and bottom groups ($p<0.05$).

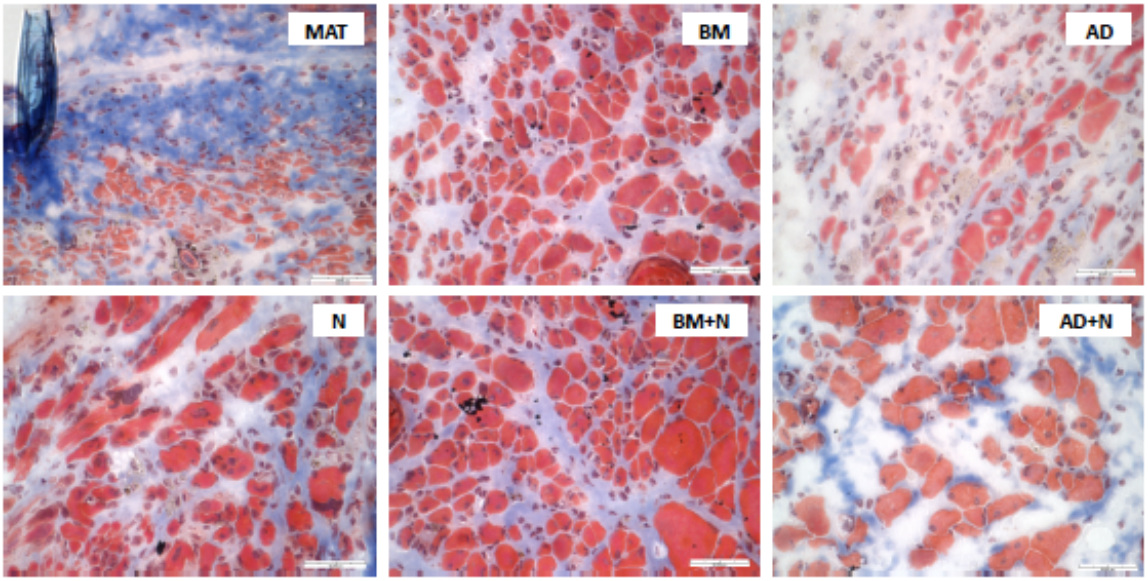

Figure 4: Histological group comparison of cellular regeneration within the implanted ECM following 42 days recovery. Representative images of all groups stained with Masson's trichrome. Note: Large white spaces with blue objects in [A] are suture holes & sutures. Magnification 400x. Scale bar = 50 µm.

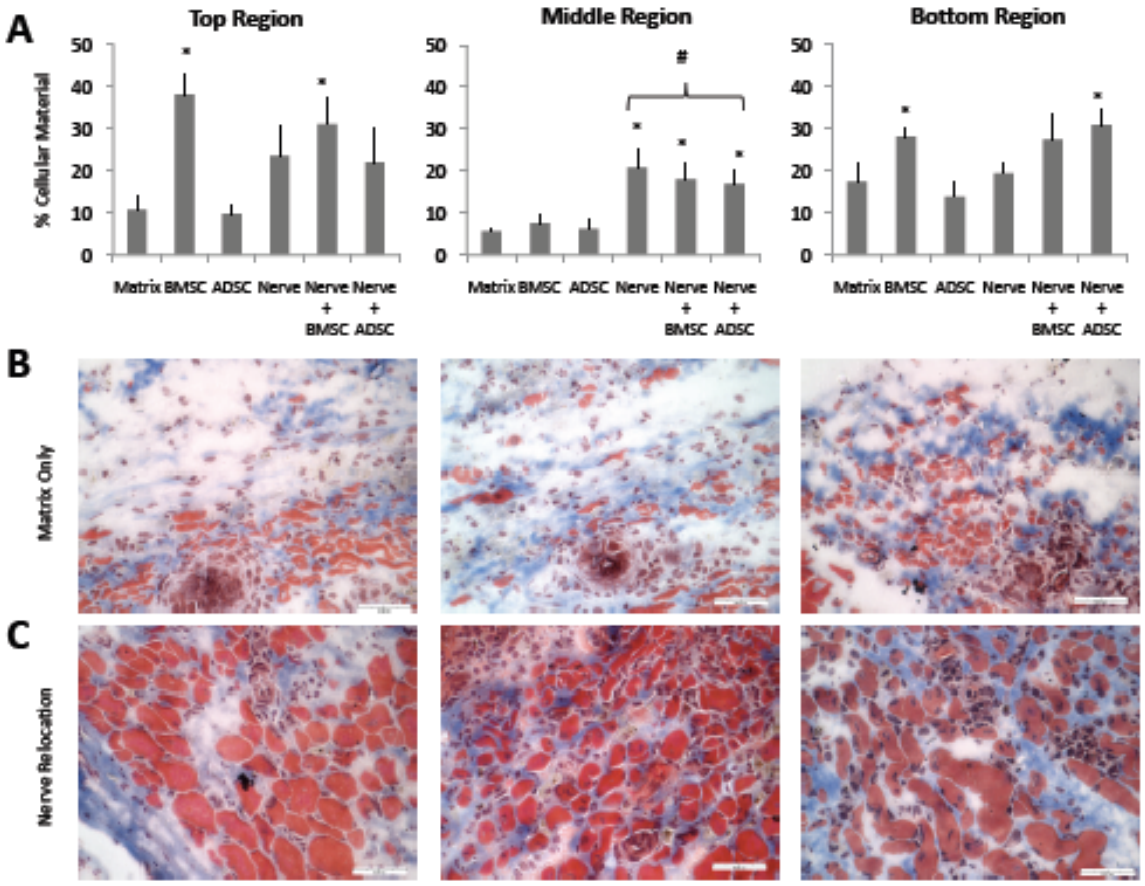

Figure 5: Histological comparison of cellular regeneration within the implanted ECM with and without nerve relocation. [A] Cellular content within the top, middle & bottom regions of the defect following 42 days recovery. Representative images of the [B] MAT group and [C] N group stained with Masson' trichrome. * Indicates statistical significance from MATRIX group ($p<0.05$). # Indicates statistical significance from all groups not involving nerve relocation ($p<0.05$). Magnification 400x. Scale bar = 50 μm.

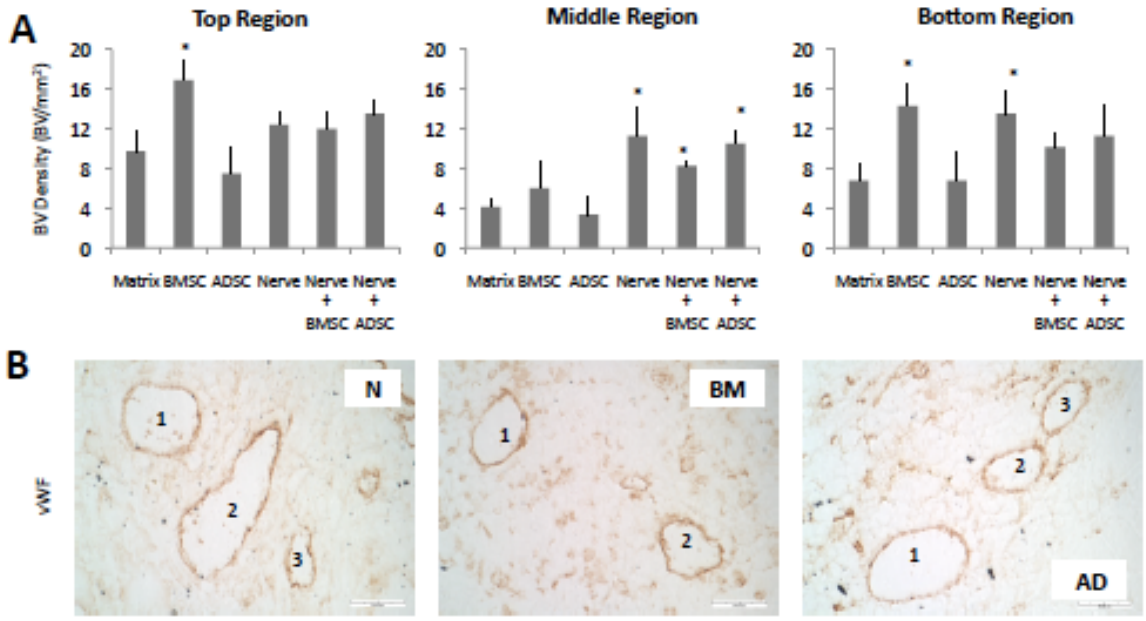

Figure 6: Histological analysis of blood vessel regeneration within the implanted ECM. [A] Blood vessel density within the top, middle & bottom regions of the defect following 42 days recovery. [B] Representative images stained with von Willebrand factor. Numbers indicate counted blood vessels meeting specified criteria: an enclosed lumen greater than 20 μm in diameter. * Indicates statistical significance from MATRIX group ($p<0.05$). Magnification 400x. Scale bar = 50 μm.

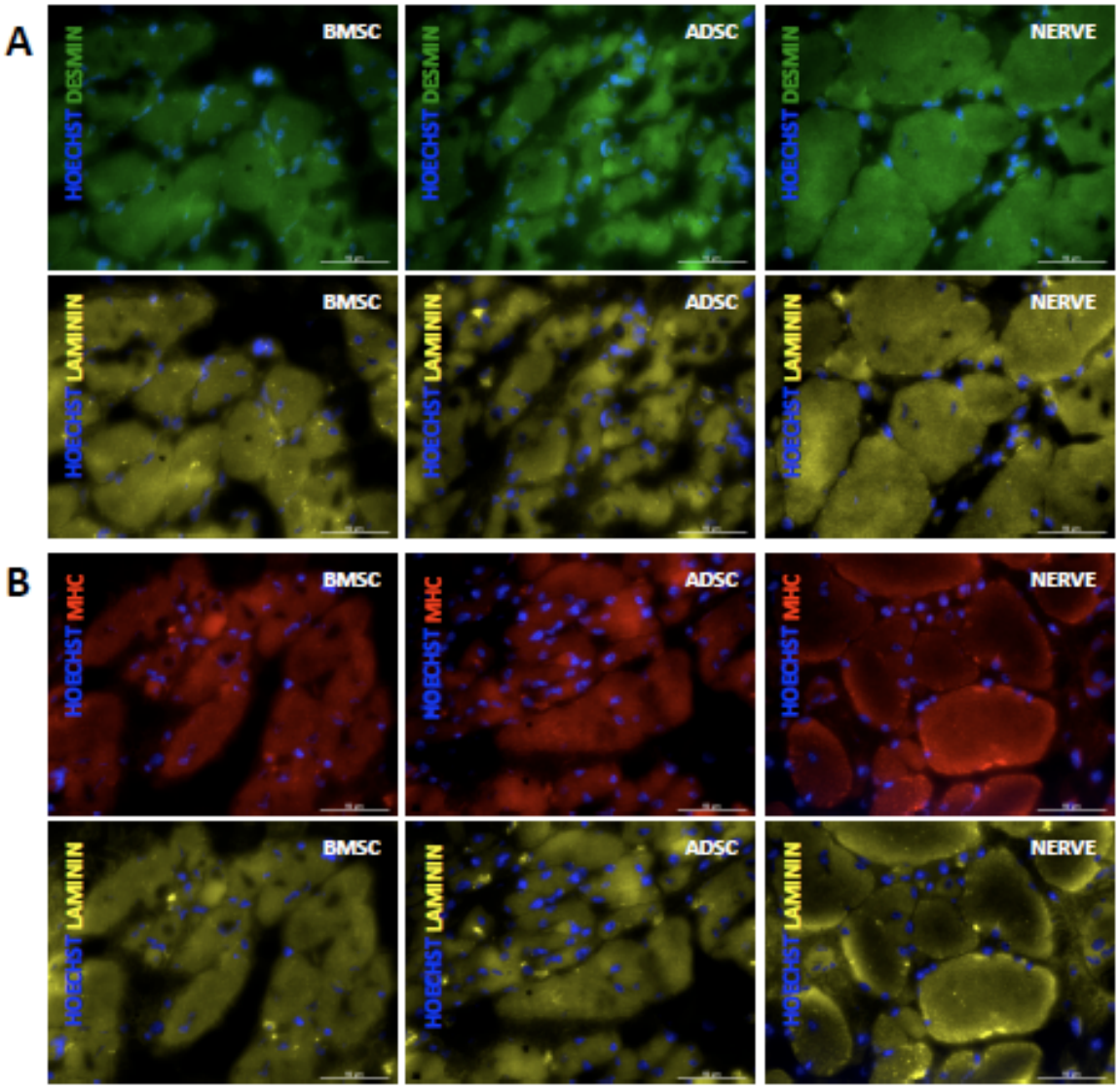

Figure 7: Immunohistochemical identification of regenerating myofibers. Representative images of desmin-, myosin heavy chain- and laminin-positive structures within the implanted ECM following 42 days recovery. Colocalization of [A] desmin/laminin and [B] MHC/laminin. Magnification 400x. Scale bar = 50 µm.

APPENDIX A: INSTRUMENTATION

A. Dual-Mode Muscle Lever System: Series 310B-LR, Aurora Scientific, Inc.

- Measurement and control of the dynamic physical properties, including length and force, of all types of muscle and connective tissue; can operate isotonically, isometrically or auxotonically.

B. Isolated Pulse Stimulator: Model 2100, A-M Systems.

- Physiological stimulation of neurological structures, used in conjunction with the dual-mode muscle lever system.

C. Rapid Sectioning Cryostat: Leica CM1900, Meyer Instruments, Inc.

- Reproducible sectioning of frozen skeletal muscle tissue for use in histological and immunohistological analysis.

D. Inverted Tissue Culture Microscope: Nikon Daiphot, Nikon Instruments, Inc.

- Magnification and visualization of histologically identifiable structures contained by frozen tissue sections obtained from the cryostat.

E. Fluorescent Microscope: Leica DM LB2, Leica Microsystems, Inc.

- Magnification and visualization of immunofluorescent structures contained by frozen tissue sections obtained from the cryostat.

F. Digital Microscope Camera: Microfire, Optronics.

- Acquisition and collection of images visualized by the Nikon Diaphot inverted tissue culture microscope.

E. Digital Microscope Camera: Leica DFC340FX, Leica Microsystems, Inc.

- Acquisition and collection of images visualized by the Leica DM LB2 fluorescent microscope.

APPENDIX B: MESENCHYMAL STEM CELL ISOLATION & CUTURE

Mesenchymal stem cell (MSC) isolation is typically based upon the selective and spontaneous adherence to the solid surface of a culturing flask. Initially, the resulting cell population is small and heterogeneous. However, this can be altered following their expansion and passaging in culture. Despite a significant amount of time spent out of their native microenvironment, differentiation can be prevented in part when grown in a control media. The resulting cell population is clinically relevant in number, homogeneous and maintains an undifferentiated state until its utilization in a therapeutic procedure.

Bone Marrow-Derived Stem Cell Isolation

Protocol

- Note strain, age, sex and weight of the animal; 2-4 mo. old animals are preferred.
- Anesthetize animals via intraperitoneal (IP) injection of sodium pentobarbital, 65 mg/kg body weight.
- Shave hind limbs and make incisions into the skin at the lateral side of the lower and upper leg parallel to the femur and tibia.
- Separate surrounding muscle groups and surgically remove the femur and tibia.
- Remove surrounding tissues from the bone and place in Dulbecco's phosphate-buffered saline (DPBS) to facilitate further cleaning.
- Place tibial and femoral bones in fresh DPBS within scientific hood and remove the epiphyses to gain access to the bone marrow cavities.
- Using an 18G needle attached to a 10 mL syringe, flush out whole bone marrow plugs using 10 mL control media per bone.
    - Control medium composed of 90% Dulbecco's modified eagle medium (DMEM) and 10% fetal bovine serum (FBS) with 1% antibiotic/antimycotic (AA) solution.
    - Place bone marrow from each bone in a 50 mL centrifuge tube.

    - Mechanically digest the bone marrow by using a series of smaller syringes to draw up and pump out control media containing bone marrow.
- Transfer media into 15 mL centrifuge tubes; centrifuge at 1000g for 5 min at 4°C.
- Aspirate supernatant and resuspend pellet with 5 mL control media.
- Plate cells in a 25 cm^2 culturing flask, incubate at 37°C and 5% CO_2.
- Following 24 hours incubation, remove the old media and replate the non-adherent fraction at a 1:2 ratio.
- Rinse initial flasks with DPBS twice to remove red blood cells (RBCs).
- Change media 24 and 48 hours following replating until cells have stabilized and begun to undertake a slightly elongated, fibroblastic morphology.
- Change media every 2-4 days until flasks have reached 80% confluency, upon which splitting procedures must be performed.

Adipose-Derived Stem Cell Isolation

Protocol

- Note strain, age, sex and weight of the animal; 2-4 mo. old animals are preferred.
- Anesthetize animals via intraperitoneal (IP) injection of sodium pentobarbital, 65 mg/kg body weight.
- Shave entire ventral side of the animal between ribs and including groin area and make a longitudinal incision, beginning at the ribs, and two bilateral incisions to expose the abdominal and pelvic cavity.
- Inject adipose tissue with epinephrine to prevent blood loss.
- Excise adipose tissue from epididymal fat pads and visceral fat surrounding the reproductive organs and kidneys.
- Rinse adipose tissue in DPBS, cut into small pieces, obtain weight of the tissue and place in a sterile 50 mL centrifuge tube under scientific hood.
- Repeat wash procedure 5-6 times until wash buffer is clear.
    - Wash with wash buffer; Hanks balanced salt solution (HBSS) containing 1% antibiotic/antimycotic (AA) solution.

    - Shake vigorously for 10 seconds, let stand until adipose floats.
    - Aspirate wash buffer using 5 mL pipette tip.
- Prepare 0.075% collagenase solution in HBSS, filter sterilize, and finally add 1% AA solution.
- Obtain weight of washed adipose tissue, then place in 150 cm^2 flask.
- Add collagenase solution to the flask and shake vigorously for 10 seconds.
- Place flask in the incubator set at 37°C and 5% CO_2; incubate for 60-90 minutes, shaking vigorously every 15 min until the tissue appears to be well-digested.
- Dispense digested tissue into two 50 mL tubes and add 20 mL control media to each tube; centrifuge at 1000g for 10 min.
- Aspirate supernatant and resuspend in 10 mL filter-sterilized cell lysis buffer containing 160 mM NH4Cl and 0.017 M Tris base, pH 7.2.
- Allow to stand for 10 min, then centrifuge at 1000g for 5 min at 4°C.
- Aspirate cell lysis buffer and resuspend pellet with 5 mL control media.
    - Control medium composed of 90% Dulbecco's modified eagle medium (DMEM) and 10% fetal bovine serum (FBS) with 1% AA solution.
- Plate cells in a 25 cm^2 culturing flask, incubate at 37°C and 5% CO_2.
- Following 24 hours incubation, remove and replace control media.
- Rinse initial flasks with DPBS twice to remove red blood cells (RBCs).
- Change media 24 and 48 hours following replating until cells have stabilized and begun to undertake a slightly elongated, fibroblastic morphology.
- Change media every 2-4 days until flasks have reached 80% confluency, upon which splitting procedures must be performed.

Mesenchymal Stem Cell Culture

Protocol

- Observe cells under the microscope and note confluency.
- If under 80% confluency:
    - Aspirate media from culture flasks using 5 mL pipette tip.

- Rinse twice with DPBS if cellular debris is present.
- Place 10 mL fresh control media in 25 cm^2 flask; 75 mL in 150 cm^2 flask.

- If at or above 80% confluency:
  - Aspirate media from culture flasks using 5 mL pipette tip.
  - Rinse twice with DPBS.
  - Place 3 mL or 15 mL 0.25% trypsin containing ethylenediaminetraacetic acid (EDTA) in a 25 cm^2 or 75 cm^2 flask and place in the incubator for 5 min.
  - Tap the flask to induce detachment of the cells from the flask bottom.
  - Remove the cell suspension and place in 15 mL sterile centrifuge tubes; obtain remaining cells by rinsing flasks twice with DPBS and aspirating the resulting suspension.
  - Centrifuge at 1000g for 5 min at 4°C.
  - Aspirate supernatant and resuspend pellet with 5 mL control media; use a 5 mL pipette tip to gently break up the pellet.
  - Split and replate the cells at a 1:3 ratio, add control media and incubate at 37°C and 5% CO_2.

APPENDIX C: EXTRACELLULAR MATRIX PREPARATION

The extracellular matrix (ECM) is derived from skeletal muscle and therefore contains complex infrastructure of this tissue, advantageous to the functional output of regenerated myofibers contained by the construct. This decellularization procedure does not significantly alter the composition of the collagenous matrix, maintaining a native microenvironment for the cells attempting to repopulate the construct.

Protocol

- Obtain medial or lateral gastrocnemius (MGAS or LGAS) muscles from an animal of the same species.
- Place in 50 mL centrifuge tubes filled with deionized water for 24 hours at 4°C.
- Replace deionized water with chloroform and continuously agitate for 72 hours at 21°C.
- Replace chloroform with 2% sodium dodecyl sulfate (SDS) and continuously agitate until all cellular material has been removed.
    - Change 2% SDS 2-3 times per week; the tissue should being to lose it color, eventually appearing white.
- Rinse the resulting extracellular matrix (ECM) in deionized water every 4-6 hours over a 48 hour period.
- Replace deionized water with a 0.1 M tris buffer solution (TBS, pH = 9.0) for 4 hours at 21°C.
- Replace TBS with phosphate buffered saline (PBS) containing 1% penicillin/streptomycin; expose the ECM to UV light for ≥12 hours and store at 4°C until its implantation.

APPENDIX D: *IN SITU* FORCE MEASUREMENTS

In situ measurements were performed on both the experimental leg and the contralateral (internal control) leg following 42 days recovery to assess the level of functional recovery within the extracellular matrix (ECM). Using the peak tension, length and weight of the lateral gastrocnemius, the cross sectional area (CSA) and specific tension (SP_0) of the muscle were calculated and expressed as a percentage of the same measurement derived from the contralateral limb.

Protocol

- Weigh animal and anesthetize via intraperitoneal (IP) injection of sodium pentobarbital, 65 mg/kg body weight.
- Shave hind limb of the experimental leg and make an incision into the skin at the lateral side of the upper thigh, perpendicular to the femur.
- Separate muscles of the upper thigh to reveal the sciatic nerve; isolate and sever the peroneal nerve, leaving intact the tibial nerve.
    - Severe the sciatic nerve as proximal as possible.
- Make bilateral incisions into the skin on the medial and lateral sides of the lower limb between the knee and ankle; remove skin and hamstring from the posterior side of the lower limb to expose the plantar flexors.
- Prevent excessive bleeding by tying off all major veins using a non-absorbable polypropylene 5-0 suture.
- Functionally isolate the lateral gastrocnemius (LGAS) by severing the branch of tibial nerve innervating the medial head of the gastrocnemius (GAS).
- Separate the posterior compartment containing the gastrocnemius, plantaris and soleus from the rest of the lower limb using tweezers; detach the calcaneus from the Achilles tendon.
- Separate the distal portion of the GAS from the plantaris and soleus.

- Insert a 1/16 inch drill bit perpendicular to the tibia into the tibial condyles.
- Place and secure the lower limb to the force measurement apparatus using the 1/16 drill bit.
- Attach the Achilles tendon using 3-0 silk thread to a servomotor muscle lever system.
    - Throughout this process, keep the LGAS wet in mineral oil and maintain muscle temperature between 36.5°C and 37.5°C using a radiant heat lamp.
- Contact the severed end of the sciatic nerve to an isolated pulse stimulator, used in conjunction with the servomotor muscle lever system.
- Adjust the muscle to optimal length with micrometer; verify by determining maximal twitch tension via submaximal stimulation at 0.5 Hz and 7 V.
    - Stimulating the muscle at various lengths while recording twitch tension will result in the development of a length-tension curve, from which the user can determine the optimal length of the muscle for maximal isometric tetanic contraction.
- Stimulate the sciatic nerve at 150 Hz and the minimum voltage necessary to elicit maximal isometric tetanic contraction.
    - After each contraction, rest the muscle for 2 min and repeat this process until the user is certain the greatest possible peak tension value has been recorded.
- Excise and record the wet weight of the as described in Appendix E, as well as the length of the lateral gastrocnemius.
- Repeat this procedure to obtain functional measurements from the contralateral leg.

APPENDIX E: TISSUE HARVESTING

Tissue Extraction & Freezing

Protocol

- Excise the lateral and medial gastrocnemius, plantaris and soleus from animal and remove excess fat or connective tissue.
- Clean and place extracted muscles in 0.9% saline solution.
- When ready to weight tissue, remove from saline solution and gently blot dry.
- Place on digital scale and record the wet weight of each tissue.
- Prepare labeled aluminum foil squares to contain each frozen tissue.
- Set up freezing apparatus by obtaining liquid nitrogen within a Styrofoam tub.
- Partially submerge a container of isopentane in the liquid nitrogen and let cool for 1-2 min, until the isopentane begins to condense.

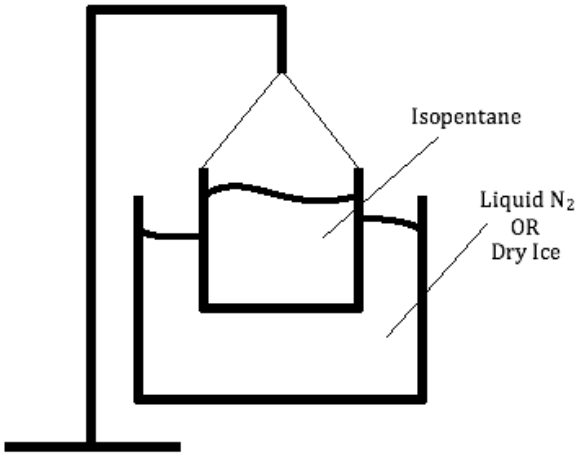

- Orient the tissue, one at a time, within an empty muscle cassette using tweezers.
- Place closed cassette in isopentane partially using large tongs, for 15 sec; longer may damage tissue while less will result in non-uniform freezing.
- Remove cassette from isopentane and transfer partially frozen muscle, using chilled tweezers, into prepared aluminum foil wrap.
- Transfer frozen tissue to -80°C freezer and store until ready for sectioning.

Tissue Sectioning

Cryostats are refrigerated chambers that contain a microtome. Here we maintain the chamber at -22°C and acquire sections 5 μm in thickness for histochemical and immunohistochemical examination. Frozen tissues have several advantages when compared to paraffin-embedded tissues, namely the speed of handling and the maintenance of enzyme and immunological functions, as fixation is unnecessary. This allows the adequate labeling of specimens using immunohistochemical techniques or fluorescent markers. There is potential for ice crystal formation during the freezing process, which may distort the image of the cell. Great care must be taken to guard against any induced artifact from the freezing process.

Protocol

- Transport frozen tissue from -80°C freezer to the cryostat and place on quick-freeze shelf, maintained at -45°C using chilled forceps.
- Using single-edge razor blades, remove healthy tissue perpendicular to existing myofibers to leave only the defected area for sectioning.
- Mount tissue onto specimen disks using optimal cutting temperature compound (OCT).
- Insert specimen disk into specimen head and orient specimen head if necessary.
- Initially adjust base of the blade holder to bring blade close to tissue using coarse feed settings and handwheel.
- Begin sectioning tissue, ensuring sections are sliding under the anti-roll plate.
    - If tissue appears shredded, (1) make sure the blade angle is set to 4.5%, (2) adjust microtome blade horizontally to work with a sharper area, and (3) replace microtome blade if necessary.
- "Grab" sectioned tissue from blade holder using a microscope slide; two tissue sections are placed on each microscope slide.
- Properly label microscope slide and place in slide holder for future use.

APPENDIX F: HISTOLOGICAL ANALYSIS

Masson's Trichrome Staining

Masson's trichrome is a three-color staining protocol used to distinguish cells from surrounding connective tissue. The recipe used here produces red keratin and muscle fibers, blue collagen and bone, light red or pink cytoplasm, and dark brown or black cell nuclei. It is applied by immersion into Bouin's solution, Weigert's iron hematoxylin, Beibrich scarlett acid fuchshin, phosphotungstic/phosphomolybdic acid, aniline blue and acetic acid.

Protocol

- Immerse slides in Bouin's solution contained in Columbia staining jars overnight; this entire protocol is performed at room temperature.
- Pour out solution and gently rinse slides with tap water.
- Immerse sections in working Weigert's iron hematoxylin for 5 min.
- Pour out solution and gently rinse slides in tap water; rinse in deionized water.
- Immerse sections in Beibrich scarlett acid fuchshin for 5 min.
- Pour out solution and gently rinse slides in tap water; rinse in deionized water.
- Immerse sections in working phosphotungstic/phosphomolybdic acid for 5 min.
- Pour out solution and immerse sections in Aniline blue for 5 min.
- Pour out solution and immerse sections in 1% acetic acid for 2 min.
- Pour out solution and gently rinse slides in tap water.
- Dehydrate sections sequentially exposing to a series of solutions for 15 sec:
    - 70% ethanol, 100% ethanol, and xylenes twice.
- Dry slides for 30 min, then mount slides by pipetting several drops of mounting medium onto slides and covering with coverslips.

Von Willebrand Staining

Von Willebrand factor (vWF) is a glycoprotein found in the blood and involved in hemostasis. Produced constitutively in the endothelium and subendothelial connective tissue, vWF can be used to identify blood vessels by staining the endothelial wall of a vessel. Here, endogenous peroxidase activity is first quenched following incubation in a peroxidase solution. A two-step biotin/avidin system is then used to increase amplification of the signal. Peroxidase-labeled streptavidin will (essentially) irreversibly bind to multiple sites on biotinylated link antibody with a high affinity. Staining is completed after incubation with a substrate-chromogen solution.

Protocol

- Immerse slides in preheated Dako target retrieval solution contained in a Coplin jar and submerged in a heated water bath for 40 min at 95-99°C.
- Remove entire jar with slides and solution; allow to cool to room temperature.
- Decant target retrieval solution, rinse slides in tris-buffered saline (0.05% Tween 20, pH 7.6, TBST) 3 times for 5 min at 21ºC.
- Dry slides for 5 min, place in humid boxes.
- Incubate sections with 3% peroxidase for 5 min at 21ºC.
- Wash slides with deionized water, then TBST; each for 5 min.
- Dry slides for 5 min, place in humid boxes.
- Incubate sections with von Willebrand factor: 1:400 in 1x phosphate-buffered saline (PBS, 1.0% BSA) for 30 min at 21ºC.
- Wash slides with TBST twice for 5 min.
- Dry slides for 5 min, place in humid boxes.
- Incubate sections with biotinylated link in PBS for 30 min at 21ºC.
- Wash slides with TBST twice for 5 min.
- Dry slides for 5 min, place in humid boxes.
- Incubate sections with streptavidin peroxidase for 30 min at 21ºC.

- Wash slides with deionized water, then TBST; each for 5 min.
- Dry slides for 5 min, place in humid boxes.
- Incubate sections with a substrate-chromogen solution for 5 min at 21ºC.
- Wash slides with tris-buffered saline (TBS), twice for 5 min.
- Dry slides for 30 min, then mount slides by pipetting several drops of mounting medium onto slides and covering with coverslips.

APPENDIX G: IMMUNOHISTOLOGICAL ANALYSIS

Indirect immunofluorescence is a technique that allows the visualization of a specific protein by binding to a specific antibody, later to be recognized by a secondary antibody chemically conjugated with to a fluorescent dye. Performed on tissue sections fixed to microscope slides, stained samples are examined under a fluorescence microscope. Upon the appropriate ultraviolet light absorption, the fluorochrome will emit its own light at a longer wavelength and allow the visualization and localization of the antibody-antigen complexes. Here we were able to simultaneously identify two primary proteins by using both fluorescein- and rhodamine-conjugated secondary antibodies. Each emit at different wavelengths, fluorescein at 495 nm and rhodamine at 570 nm. Additionally, sections were incubated with Hoechst 33258 as it emits at 395 nm. These different excitation wavelengths allowed us to separately image all proteins and overlay those images, creating a composite image spatially locating all three proteins.

Blocking agents bovine serum albumin (BSA) and normal serum derived from the source of the primary antibody were used to inhibit non-specific binding of antibodies during staining procedures. Additionally, BSA served to stabilize enzymes and enzymatic reactions while preventing adhesion of enzymes to equipment surfaces.

Desmin is an early structural cytoskeletal protein arranged in a sarcomeric fashion within a myofiber. Although present in small quantities during early stages of muscle development, its expression increases as the cell nears terminal differentiation and can be used to identify mature muscle cells (Bornemann & Schmalbruch 1992). Myosin heavy chain (MHC) is a highly conserved and ubiquitously expressed motor protein present in skeletal muscle. Composing part of the sarcomere, it can be used to identify mature myofibers that are well developed

and capable of contraction. Laminin is a structural non-collagenous glycoprotein and a major component of the basal lamina surrounding a myofiber. Its presence along the entire boundary of a myofiber does much to substantiate this identity. Finally, central nuclei are well-known characteristic of newly regenerating myofibers and can be identified, along with all nuclei, by Hoechst 33258, a fluorescent DNA-binding compound.

Protocol

- Begin antigen exposure and retrieval by immersing slides in 2 M hydrochloric acid (HCl) for 45 minutes at 21ºC.
- Immerse slides in tris-buffered saline (0.1% Tween 20, TBST) for 30 min at 21ºC.
- Immerse slides in 10% normal serum in 1x TBS (1.0% BSA) for 2 hours at 21ºC.
- Dry slides for 5 min, place in humid boxes to prevent drying during incubation
- Incubate sections with chosen primary antibody for 2 hours at 21ºC:
    - Desmin, goat polyclonal IgG: 1:400 in 1x phosphate-buffered saline (PBS, 1.0% BSA).
    - Myosin Heavy Chain (MHC), goat polyclonal IgG: 1:400 in 1x PBS (1.0% BSA).
- Wash slides with TBST, 3 times for 5 min.
- Dry slides for 5 min, place in humid boxes.
- Incubate sections with $F(ab')_2$ donkey anti-goat IgG fluorescein: 1:200 in PBS for 60 min at 21ºC (slides must be protected from light from this point forward).
- Wash slides with TBST, 3 times for 5 min.
- Dry slides for 5 min, place in humid boxes.
- Incubate sections with laminin, mouse monoclonal IgG: 1:400 in 1x PBS (1.0% BSA) for 2 hours at 21ºC.
- Wash slides with TBST, 3 times for 5 min.
- Dry slides for 5 min, place in humid boxes.

- Incubate sections with $F(ab')_2$ donkey anti-mouse IgG rhodamine: 1:200 in PBS for 60 min at 21ºC.
- Wash slides with TBST, 3 times for 5 min.
- Dry slides for 5 min, place in humid boxes.
- Incubate sections with Hoechst 33258 (pentahydrate bis-benzimide, 1:1000 H_2O) for 45 min at 21ºC.
- Wash slides with tris-buffered saline (TBS), 3 times for 5 min.
- Dry slides for 30 min, then mount slides by pipetting several drops of mounting medium onto slides and covering with coverslips.

APPENDIX H: RAW DATA

Mass & Force Measurement Data

Animal	Group	Mass: Surgery (g)	Mass: Cells (g)	Mass: Nerve (g)	Mass: FM (g)
Matrix Only					
M003	M	485	---	---	541
M009	M	496	---	---	565
M010	M	504	---	---	536
M014	M	533	---	---	520
M016	M	510	---	---	560
M030	M	552	---	---	576
M031	M	565	---	---	615
M033	M	551	---	---	600
Mean:		**524.5**	**---**	**---**	**564.1**
SEM:		**10.5**	**---**	**---**	**11.4**
M008	B	453	451	---	449
M017	B	512	513	---	562
M018	B	508	493	---	551
M021	B	449	510	---	549
M058	B	531	568	---	597
M059	B	568	520	---	538
Mean:		**503.5**	**509.2**	**---**	**541.0**
SEM:		**18.7**	**15.5**	**---**	**20.2**
M043	A	503	502	---	537
M044	A	546	542	---	577
M047	A	539	572	---	605
M048	A	518	578	---	543
M060	A	585	591	---	602
M061	A	576	578	---	591
Mean:		**544.5**	**560.5**	**---**	**575.8**
SEM:		**13.0**	**13.5**	**---**	**12.0**

Animal	Group	Mass: Surgery (g)	Mass: Cells (g)	Mass: Nerve (g)	Mass: FM (g)
Nerve Relocation					
M019	N	522	---	552	563
M020	N	468	---	486	502
M023	N	491	---	510	509
M025	N	562	---	579	580
M026	N	532	---	539	466
M027	N	555	---	561	581
M028	N	444	---	484	487
M029	N	612	---	609	589
Mean:		**523.3**	**---**	**540.0**	**534.6**
SEM:		**19.3**	**---**	**15.7**	**17.3**
BMSC Injection + Nerve Relocation					
M024	BN	530	529	542	549
M034	BN	460	497	534	545
M035	BN	502	525	546	549
M036	BN	484	482	508	517
M041	BN	520	532	548	572
M042	BN	465	474	486	502
M052	BN	520	509	527	531
M053	BN	504	496	515	527
Mean:		**498.1**	**505.5**	**525.8**	**536.5**
SEM:		**9.2**	**7.7**	**7.6**	**7.7**
ADSC Injection + Nerve Relocation					
M039	AN	497	491	510	523
M040	AN	560	565	590	615
M045	AN	565	563	565	597
M051	AN	566	556	587	587
M054	AN	518	576	539	558
M055	AN	520	514	528	548
M056	AN	518	514	534	545
Mean:		**534.9**	**539.9**	**550.4**	**567.6**
SEM:		**10.6**	**12.4**	**11.6**	**12.4**

Defect (Left) Leg

Defect Mass (mg)	Def LGAS Mass (mg)	Def MGAS Mass (mg)	Def SOL Mass (mg)	Def PLAN Mass (mg)	Def LGAS Length (mm)
Matrix Only					
149	1287	1065	248	462	30
188	1357	1338	263	597	31
177	1232	1138	237	501	27
193	1212	1118	227	475	27
195	1181	1123	225	504	28
191	1255	1214	244	488	30
164	1266	1239	220	517	31
206	1393	1178	238	535	31
182.9	**1272.9**	**1176.6**	**237.8**	**509.9**	**29.4**
6.6	**25.3**	**30.4**	**5.0**	**14.9**	**0.6**
BMSC Injection					
179	1070	1011	222	478	26
180	1288	1213	277	482	29
205	1298	1212	284	527	28
212	1154	1133	222	500	29
190	1186	1142	218	515	30
224	1175	1125	239	509	30
198.3	**1195.2**	**1139.3**	**243.7**	**501.8**	**28.7**
7.5	**35.1**	**30.2**	**12.1**	**7.8**	**0.6**
ADSC Injection					
186	1190	1164	198	511	30
188	1227	1417	224	564	30
155	1427	1347	278	590	31
149	1378	1198	202	537	32
184	1116	1058	208	557	30
217	1239	1097	262	490	30
179.8	**1262.8**	**1213.5**	**228.7**	**541.5**	**30.5**
10.1	**47.9**	**57.6**	**13.7**	**14.9**	**0.3**

Defect (Left) Leg

Defect Mass (mg)	Def LGAS Mass (mg)	Def MGAS Mass (mg)	Def SOL Mass (mg)	Def PLAN Mass (mg)	Def LGAS Length (mm)
Nerve Relocation					
170	1352	1363	228	550	30
218	1260	1130	216	469	26
178	1252	1154	228	425	27
188	1209	1113	236	429	28
159	1046	1083	226	450	28
186	1430	1312	247	544	30
175	1117	1006	207	430	28
190	1301	1200	257	518	31
183.0	**1245.9**	**1170.1**	**230.6**	**476.9**	**28.5**
6.2	**43.6**	**41.8**	**5.7**	**18.7**	**0.6**
BMSC Injection + Nerve Relocation					
159	1407	1123	204	471	29
158	1231	1134	238	500	30
176	1274	1186	193	505	32
187	1265	1193	270	486	32
167	1254	1234	232	554	31
180	1137	917	184	435	29
143	1247	1178	225	516	31
147	1091	1103	191	470	31
164.6	**1238.3**	**1133.5**	**217.1**	**492.1**	**30.6**
5.6	**33.5**	**34.4**	**10.4**	**12.6**	**0.4**
ADSC Injection + Nerve Relocation					
181	1121	1164	224	464	32
149	1304	1267	255	514	31
153	1564	1476	258	570	32
177	1549	1153	230	534	33
222	1326	1234	275	543	32
207	1193	1052	203	486	30
189	1277	1192	189	481	31
182.6	**1333.4**	**1219.7**	**233.4**	**513.1**	**31.6**
10.0	**63.4**	**49.9**	**11.7**	**14.4**	**0.4**

Def LGAS CSA (cm^2)	Def Tetanic Force (N)	Optimal Length (N)	Def Max Force (N)	Def Specific Tension (N/cm^2)
Matrix Only				
1.06	17.11	0.68	16.43	15.54
1.08	19.70	0.67	19.03	17.64
1.12	18.85	0.64	18.21	16.20
1.11	20.87	0.72	20.15	18.22
1.04	17.29	0.67	16.62	15.99
1.03	16.76	0.63	16.13	15.65
1.01	16.72	0.64	16.08	15.98
1.11	18.14	0.67	17.47	15.78
1.1	**18.2**	**0.7**	**17.5**	**16.4**
0.0	**0.5**	**0.0**	**0.5**	**0.4**
BMSC Injection				
1.01	19.16	0.69	18.47	18.22
1.09	21.94	0.71	21.23	19.40
1.14	20.63	0.64	19.99	17.50
0.98	18.07	0.67	17.40	17.75
0.97	19.84	0.62	19.22	19.73
0.97	20.13	0.66	19.47	20.18
1.0	**20.0**	**0.7**	**19.3**	**18.8**
0.0	**0.5**	**0.0**	**0.5**	**0.5**
ADSC Injection				
0.98	16.35	0.62	15.73	16.09
1.01	17.16	0.62	16.54	16.41
1.13	18.95	0.65	18.30	16.14
1.06	19.93	0.62	19.31	18.20
0.92	13.72	0.65	13.07	14.26
1.02	16.59	0.62	15.97	15.69
1.0	**17.1**	**0.6**	**16.5**	**16.1**
0.0	**0.9**	**0.0**	**0.9**	**0.5**

Def LGAS CSA (cm^2)	Def Tetanic Force (N)	Optimal Length (N)	Def Max Force (N)	Def Specific Tension (N/cm^2)
Nerve Relocation				
1.11	21.18	0.64	20.54	18.50
1.19	20.85	0.66	20.19	16.91
1.14	18.35	0.64	17.71	15.50
1.06	22.49	0.68	21.81	20.50
0.92	18.14	0.67	17.47	18.98
1.17	22.68	0.63	22.05	18.77
0.98	17.88	0.66	17.22	17.52
1.03	20.65	0.64	20.01	19.35
1.1	**20.3**	**0.7**	**19.6**	**18.3**
0.0	**0.7**	**0.0**	**0.7**	**0.6**
BMSC Injection + Nerve Relocation				
1.20	23.91	0.64	23.27	19.47
1.01	21.03	0.64	20.39	20.17
0.98	17.43	0.59	16.84	17.17
0.97	17.43	0.62	16.81	17.26
1.00	20.78	0.69	20.09	20.16
0.97	15.44	0.63	14.81	15.33
0.99	21.13	0.66	20.47	20.65
0.87	18.64	0.62	18.02	20.78
1.0	**19.5**	**0.6**	**18.8**	**18.9**
0.0	**1.0**	**0.0**	**1.0**	**0.7**
ADSC Injection + Nerve Relocation				
0.86	16.16	0.62	15.54	18.00
1.04	19.24	0.62	18.62	17.97
1.20	25.70	0.63	25.07	20.82
1.16	17.36	0.68	16.68	14.42
1.02	21.37	0.63	20.74	20.31
0.98	19.59	0.65	18.94	19.33
1.01	18.04	0.64	17.40	17.14
1.0	**19.6**	**0.6**	**19.0**	**18.3**
0.0	**1.2**	**0.0**	**1.2**	**0.8**

Contralateral/Control (Right) Leg

Con LGAS Mass (mg)	Con MGAS Mass (mg)	Con SOL Mass (mg)	Con PLAN Mass (mg)	Con LGAS Length (mm)
Matrix Only				
1224	1018	179	449	30
1402	1168	227	552	32
1299	1084	211	477	28
1287	1095	212	443	28
1209	1076	216	471	28
1275	1188	180	463	31
1282	1186	258	519	31
1330	1112	192	458	31
1288.5	**1115.9**	**209.4**	**479.0**	**29.9**
21.3	**21.3**	**9.3**	**13.3**	**0.6**
BMSC Injection				
1092	979	176	406	28
1352	1110	201	479	27
1305	1151	191	522	28
1163	1032	195	445	28
1287	1148	206	516	30
1183	1012	200	435	30
1230.3	**1072.0**	**194.8**	**467.2**	**28.5**
40.6	**30.2**	**4.3**	**19.0**	**0.5**
ADSC Injection				
1187	1034	190	478	30
1385	1234	206	481	30
1438	1232	214	518	30
1345	1095	201	426	31
1310	1100	206	509	31
1283	1178	477	206	31
1324.7	**1145.5**	**249.0**	**436.3**	**30.5**
35.5	**33.4**	**45.7**	**47.9**	**0.2**

Contralateral/Control (Right) Leg

Con LGAS Mass (mg)	Con MGAS Mass (mg)	Con SOL Mass (mg)	Con PLAN Mass (mg)	Con LGAS Length (mm)
Nerve Relocation				
1497	1201	216	532	30
1181	1051	206	452	26
1223	1054	187	434	28
1378	1228	190	486	29
1229	1114	218	439	30
1531	1340	248	542	31
1194	1057	235	432	29
1221	1160	258	490	30
1306.8	**1150.6**	**219.8**	**475.9**	**29.1**
50.1	**36.3**	**9.1**	**15.5**	**0.5**
BMSC Injection + Nerve Relocation				
1272	1072	206	466	29
1354	1104	217	510	31
1230	1107	194	429	32
1167	1079	185	431	30
1429	1269	260	555	33
1126	1044	186	417	27
1229	1095	193	449	30
1165	1075	203	446	29
1246.5	**1105.6**	**205.5**	**462.9**	**30.1**
36.2	**24.4**	**8.7**	**16.6**	**0.7**
ADSC Injection + Nerve Relocation				
1255	1153	180	443	31
1334	1190	207	523	31
1396	1261	210	502	32
1516	1332	174	512	30
1295	1130	223	477	33
1182	1005	188	445	31
1361	1192	206	463	31
1334.1	**1180.4**	**198.3**	**480.7**	**31.3**
40.4	**39.0**	**6.7**	**12.2**	**0.4**

Con LGAS CSA (cm^2)	Def Tetanic Force (N)	Optimal Length (N)	Def Max Force (N)	Con Specific Tension (N/cm^2)
Matrix Only				
1.01	18.20	0.67	17.53	17.44
1.08	20.02	0.69	19.33	17.91
1.14	20.98	0.65	20.33	17.79
1.13	23.08	0.68	22.40	19.78
1.06	25.31	0.69	24.62	23.14
1.01	24.08	0.68	23.40	23.09
1.02	21.44	0.65	20.79	20.40
1.06	19.59	0.69	18.90	17.88
1.1	**21.6**	**0.7**	**20.9**	**19.7**
0.0	**0.9**	**0.0**	**0.9**	**0.8**
BMSC Injection				
0.96	19.44	0.71	18.73	19.49
1.23	22.94	0.68	22.26	18.04
1.15	23.73	0.65	23.08	20.10
1.02	20.86	0.64	20.22	19.76
1.06	21.72	0.61	21.11	19.97
0.97	20.73	0.64	20.09	20.68
1.1	**21.6**	**0.7**	**20.9**	**19.7**
0.0	**0.6**	**0.0**	**0.6**	**0.4**
ADSC Injection				
0.97	18.77	0.65	18.12	18.59
1.14	23.44	0.67	22.77	20.02
1.18	23.50	0.64	22.86	19.36
1.07	22.00	0.66	21.34	19.96
1.04	21.67	0.69	20.98	20.15
1.02	20.28	0.64	19.64	19.26
1.1	**21.6**	**0.7**	**21.0**	**19.6**
0.0	**0.8**	**0.0**	**0.7**	**0.2**

Con LGAS CSA (cm^2)	Def Tetanic Force (N)	Optimal Length (N)	Def Max Force (N)	Con Specific Tension (N/cm^2)
Nerve Relocation				
1.23	23.32	0.67	22.65	18.42
1.12	20.74	0.65	20.09	17.95
1.08	19.35	0.62	18.73	17.40
1.17	24.99	0.68	24.31	20.76
1.01	21.87	0.64	21.23	21.03
1.22	24.00	0.65	23.35	19.19
1.01	22.60	0.63	21.97	21.66
1.00	20.61	0.65	19.96	19.90
1.1	**22.2**	**0.6**	**21.5**	**19.5**
0.0	**0.7**	**0.0**	**0.7**	**0.5**
BMSC Injection + Nerve Relocation				
1.08	22.00	0.63	21.37	19.77
1.08	20.65	0.59	20.06	18.64
0.95	19.53	0.62	18.91	19.97
0.96	19.92	0.64	19.28	20.12
1.07	20.25	0.65	19.60	18.37
1.03	21.23	0.69	20.54	19.99
1.01	19.35	0.65	18.70	18.53
0.99	22.56	0.71	21.85	22.08
1.0	**20.7**	**0.6**	**20.0**	**19.7**
0.0	**0.4**	**0.0**	**0.4**	**0.4**
ADSC Injection + Nerve Relocation				
1.00	19.68	0.71	18.97	19.02
1.06	19.35	0.67	18.68	17.62
1.07	24.24	0.66	23.58	21.94
1.25	25.02	0.62	24.40	19.60
0.97	19.68	0.65	19.03	19.68
0.94	17.92	0.62	17.30	18.41
1.08	22.60	0.64	21.96	20.30
1.1	**21.2**	**0.7**	**20.6**	**19.5**
0.0	**1.0**	**0.0**	**1.0**	**0.5**

LGAS Mass (% Contralateral)	Def Force (% Contralateral)	Specific Tension (% Contralateral)
Matrix Only		
105.1	94.0	89.1
96.8	98.4	98.5
94.8	89.8	91.1
94.2	90.4	92.1
97.7	68.3	69.1
98.4	69.6	67.8
98.8	78.0	78.3
104.7	92.6	88.3
98.8	**85.1**	**84.3**
1.5	**4.1**	**4.0**
BMSC Injection		
98.0	98.6	93.5
95.3	95.6	107.5
99.5	86.9	87.1
99.2	86.6	89.8
92.2	91.3	98.8
99.3	97.1	97.6
97.2	**92.7**	**95.7**
1.2	**2.1**	**3.0**
ADSC Injection		
100.3	87.1	86.6
88.6	73.2	82.0
99.2	80.6	83.4
102.5	90.6	91.2
85.2	63.3	70.8
96.6	81.8	81.5
95.4	**79.4**	**82.6**
2.8	**4.0**	**2.8**

LGAS Mass (% Contralateral)	Def Force (% Contralateral)	Specific Tension (% Contralateral)
Nerve Relocation		
90.3	90.8	100.4
106.7	100.5	94.2
102.4	94.8	89.1
87.7	90.0	98.7
85.1	82.9	90.2
93.4	94.5	97.8
93.6	79.1	80.9
106.6	100.2	97.2
95.7	**91.6**	**93.6**
3.0	**2.7**	**2.3**
BMSC Injection + Nerve Relocation		
110.6	108.7	98.4
90.9	101.8	108.2
103.6	89.2	86.0
108.4	87.5	85.8
87.8	102.6	109.7
101.0	72.7	76.7
101.5	109.2	111.5
93.6	82.6	94.1
99.7	**94.3**	**96.3**
2.9	**4.7**	**4.6**
ADSC Injection + Nerve Relocation		
89.3	82.1	94.7
97.8	99.4	102.0
112.0	106.0	94.9
102.2	69.4	73.6
102.4	108.6	103.2
100.9	109.3	105.0
93.8	79.8	84.4
99.8	**93.5**	**94.0**
2.7	**6.1**	**4.3**

Masson's Trichrome Quantification

		Image: Muscle (%)			Defect: Muscle (%)		
Animal	Image	Top	Mid	Bot	Top	Mid	Bot
Matrix Only							
M030	1	15.3	4.4	24.0	14.6	7.1	24.8
	2	13.7	6.6	22.1			
	3	14.9	10.4	28.4			
M031	1	11.3	4.5	11.3	13.1	5.7	17.8
	2	14.9	8.9	18.7			
	3	13.1	3.7	23.5			
M033	1	6.7	2.8	8.0	4.5	4.3	9.6
	2	1.9	5.0	9.8			
	3	5.0	5.1	10.9			
Ave:					**10.7**	**5.7**	**17.4**
SEM:					**3.1**	**0.8**	**4.4**
BMSC Injection							
M021	1	44.5	5.5	24.7	42.6	5.8	27.7
	2	56.7	6.9	22.5			
	3	26.6	5.1	35.8			
M058	1	31.5	9.4	31.4	43.3	12.1	31.3
	2	47.1	15.0	30.8			
	3	51.2	11.8	31.8			
M059	1	18.6	1.0	29.9	28.2	4.8	25.2
	2	33.6	0.9	17.8			
	3	32.6	12.3	27.9			
Ave:					**38.0**	**7.5**	**28.1**
SEM:					**4.9**	**2.3**	**1.8**
ADSC Injection							
M043	1	4.2	2.9	29.1	6.0	3.6	20.5
	2	7.5	5.3	23.0			
	3	6.4	2.5	9.5			
M047	1	10.5	10.1	7.4	11.8	10.7	7.4
	2	22.7	7.5	7.5			
	3	2.0	14.7	7.4			
M060	1	12.1	3.5	15.0	11.5	4.2	13.1
	2	10.5	6.1	14.9			
	3	11.8	3.0	9.5			
Ave:					**9.7**	**6.2**	**13.7**
SEM:					**1.9**	**2.3**	**3.8**

		Image: Muscle (%)			Defect: Muscle (%)		
Animal	Image	Top	Mid	Bot	Top	Mid	Bot
Nerve Relocation							
M025	1	29.4	21.1	16.9	26.7	21.3	20.6
	2	28.5	22.6	20.3			
	3	22.2	20.2	24.6			
M027	1	17.9	8.8	19.5	10.1	12.7	14.9
	2	3.1	13.2	12.7			
	3	9.5	16.2	12.5			
M028	1	37.1	29.4	20.9	33.6	28.6	22.5
	2	15.1	35.5	21.6			
	3	48.6	21.0	25.1			
Ave:					**23.5**	**20.9**	**19.3**
SEM:					**7.0**	**4.6**	**2.3**
BMSC Injection + Nerve Injection							
M041	1	15.8	9.6	24.8	18.8	14.8	37.8
	2	16.9	17.0	41.8			
	3	23.6	17.7	46.8			
M042	1	46.1	28.8	27.0	38.0	25.7	26.3
	2	35.9	21.5	25.5			
	3	32.1	27.0	26.3			
M052	1	50.4	15.1	21.7	35.9	13.7	17.9
	2	28.0	12.0	18.7			
	3	29.4	13.9	13.4			
Ave:					**30.9**	**18.1**	**27.3**
SEM:					**6.1**	**3.8**	**5.8**
ADSC Injection + Nerve Injection							
M039	1	10.1	17.2	26.6	6.3	15.4	24.8
	2	4.2	16.2	32.2			
	3	4.4	12.7	15.5			
M054	1	14.5	15.5	37.5	33.5	12.2	36.7
	2	40.0	9.1	34.2			
	3	45.9	12.1	38.3			
M055	1	15.7	25.1	30.9	26.3	23.3	30.8
	2	27.0	20.7	39.8			
	3	36.1	24.0	21.8			
Ave:					**22.0**	**17.0**	**30.8**
SEM:					**8.1**	**3.3**	**3.4**

Animal	Region	Image: Muscle (%)
Control Muscle		
M031	M	96.8
M021	B	98.5
M021	M	99.5
M021	T	98.9
M025	T	96.8
M041	T	99.6
M041	B	95.8
M039	T	97.2
M043	T	99.0
M047	B	98.8
M058	M	96.9
M058	T	95.3
Ave:		**97.6**
SEM:		**0.5**

Von Willebrand Factor Quantification

		BV Count - Image			BV/mm^2 - Defect		
Animal	Image	Top	Mid	Bot	Top	Mid	Bot
Matrix Only							
M030	1	5	2	3	13.5	5.6	9.0
	2	3	1	2			
	3	4	2	3			
M031	1	2	1	2	6.8	3.4	7.9
	2	3	0	1			
	3	1	2	4			
M033	1	3	1	2	9.0	3.4	3.4
	2	3	1	0			
	3	2	1	1			
Ave:					**9.8**	**4.1**	**6.8**
SEM:					**2.0**	**0.8**	**1.7**
BMSC Injection							
M021	1	5	1	5	13.5	2.3	15.8
	2	2	1	5			
	3	5	0	4			
M058	1	7	2	3	20.3	11.3	10.2
	2	5	4	3			
	3	6	4	3			
M059	1	4	1	5	16.9	4.5	16.9
	2	4	1	6			
	3	7	2	4			
Ave:					**16.9**	**6.0**	**14.3**
SEM:					**2.0**	**2.7**	**2.1**
ADSC Injection							
M043	1	5	1	6	12.4	6.8	12.4
	2	4	3	3			
	3	2	2	2			
M047	1	2	2	3	6.8	2.3	4.5
	2	1	0	0			
	3	3	0	1			
M060	1	2	0	1	3.4	1.1	3.4
	2	1	1	1			
	3	0	0	1			
Ave:					**7.5**	**3.4**	**6.8**
SEM:					**2.6**	**1.7**	**2.8**

		BV Count - Image			BV/mm^2 - Defect		
Animal	Image	Top	Mid	Bot	Top	Mid	Bot
Nerve Relocation							
M025	1	5	2	4	12.4	5.6	11.3
	2	3	1	3			
	3	3	2	3			
M027	1	5	4	5	14.7	15.8	18.1
	2	4	5	7			
	3	4	5	4			
M028	1	2	3	0	10.2	12.4	11.3
	2	3	4	4			
	3	4	4	6			
Ave:					**12.4**	**11.3**	**13.5**
SEM:					**1.3**	**3.0**	**2.3**
BMSC Injection + Nerve Injection							
M041	1	5	3	2	14.7	7.9	10.2
	2	2	2	5			
	3	6	2	2			
M042	1	6	4	5	12.4	7.9	12.4
	2	2	2	3			
	3	3	1	3			
M052	1	4	3	3	9.0	9.0	7.9
	2	2	3	1			
	3	2	2	3			
Ave:					**12.0**	**8.3**	**10.2**
SEM:					**1.6**	**0.4**	**1.3**
ADSC Injection + Nerve Injection							
M039	1	4	6	3	11.3	12.4	15.8
	2	3	2	5			
	3	3	3	6			
M054	1	3	1	2	15.8	7.9	5.6
	2	4	3	2			
	3	7	3	1			
M055	1	5	2	4	13.5	11.3	12.4
	2	5	3	2			
	3	2	5	5			
Ave:					**13.5**	**10.5**	**11.3**
SEM:					**1.3**	**1.4**	**3.0**

REFERENCES

Al-Khaldi A, Eliopoulos N, Martineau D, Lejeune L, Lachapelle K, Galipeau J. (2003) Postnatal bone marrow stromal cells elicit a potent VEGF-dependent neoangiogenic response in vivo. *Gene Ther*. 10(8): 621–9.

Anderson DJ, Gage FH, Weissman IL. (2001) Can stem cells cross lineage boundaries? *Nature Med*. 7: 393-395.

Arnold L, Henry A, Poron F, Bab-Amer Y, van Rooijen N, Plonquet A, Gherardi RK, Chazaud B. (2007) Inflammatory monocytes recruited after skeletal muscle injury switch into anti-inflammatory macrophages to support myogenesis. *J Exp Med*. 204(5): 1057-1069.

Asakura A, Komaki M, Rudnicki MA. (2001) Muscle satellite cells are multipotential stem cells that exhibit myogenic, osteogenic and adipogenic differentiation. *Differentiation*. 68: 245-253.

Badylak SF. (2007) The extracellular matrix as a biologic scaffold material. *Biomater*. 28(25): 3587-3593.

Bixby JL, Van Essen DC. (1979) Competition between foreign and original nerves in adult mammalian skeletal muscle. *Nature*. 282: 726-729.

Borisov AB, Dedkov EI, Carlson BM. (2001) Interrelations of myogenic response, progressive atrophy of muscle fibers, and cell death in denervated skeletal muscle. *Anat Rec*. 264: 203-218.

Borisov AB, Dedkov EI, Carlson BM. (2005) Abortive myogenesis in denervated skeletal muscle: differentiative properties of satellite cells, their migration, and block of terminal differentiation. *Anat Embryol*. 209: 269-279.

Borschel GH, Dennis RG, Kuzon WM. (2004) Contractile skeletal muscle tissue-engineered on an acellular scaffold. *Plast Reconstr Surg*. 113: 595-602.

Chakravarthy MV, Spangenburg EE, Booth FW. (2001) Culture in low levels of oxygen enhances in vitro proliferation potential of satellite cells from old skeletal muscles. *Cell Mol Life Sci*. 58: 1150-1158.

Charge SBP, Rudnicki MA. (2004) Cellular and molecular regulation of muscle regeneration. *Physiol Rev*. 84: 209-238.

Csete M, Walikonis J, Slawny N, Wei Y, Korsnes S, Doyle JC, Wold B. (2001) Oxygen-mediated regulation of skeletal muscle satellite cell proliferation and adipogenesis in culture. *J Cell Physiol*. 189: 189-196.

Deponti D, Buono R, Cafanzaro G, De Palma C, Longhi R, Meneveri F, Bresolin N, Bass MT, Cossu G, Clementi E, Brunelli S. (2009) The low affinity receptor for neurotrophins p57NTR plays a key role for satellite cell function in muscle repair acting via RhoA. *Mol Biol Cell*. Published online June 24, 2009.

Dezawa M, Ishikawa H, Itokazu Y, Yoshihara T, Hoshino M, Takeda S, Ide C, Nabeshima Y. (2005) Bone marrow stromal cells generate muscle cells and repair muscle degeneration. *Science*. 309(5732): 314-317.

Di Carlo A, De Mori R, Martelli F, Pompilio G, Capogrossi MC, Germani A. (2004) Hypoxia inhibits myogenic differentiation through accelerated MyoD degradation. *J Biol Chem*. 279: 16332-16338.

Donovan MJ, Miranda RC, Kraerner R, McCaffrey TA, Tessarolo L, Mahadeo D, Sharif S, Kaplan DR, Tsoulfas P, Parada L, Toran-Allerand CD, Haijar DP, Hempstead BL. (1995) Neurotrophin and neurotrophin receptors in vascular smooth muscle cells. *Am J Pathol*. 147: 309-324.

Emanueli C, Salis MB, Pinna A, Graiani G, Manni L, Madeddu P. (2002) Nerve growth factor promotes angiogenesis and arteriogenesis in ischemic hindlimbs. *Circulation*. 106: 2257-2262.

Engler AJ, Sen S, Sweeney HL, Discher DE. (2006) Matrix elasticity directs stem cell lineage specification. *Cell*. 126: 677-689.

Engler AJ, Griffin MA, Sen S, Bonnemann CG, Sweeney HL, Discher DE. (2004) Myotubes differentiate optimally on substrates with tissue-like stiffness: pathological implications for soft or stiff microenvironments. *J Cell Biol*. 166(6): 877-887.

Ferrari G, Cusella–De Angelis G, Coletta M, Paolucci E, Stornaiuolo A, Cossu G, Mavilio F. (1998) Muscle regeneration by bone marrow-derived myogenic progenitors. *Science*. 279: 1528-1530.

Friedenstein AJ, Chailakhjan RK, Lalykina KS. (1970) The development of fibroblas colonies in monolayer cultures of guinea pig bone marrow and spleen cells. *Cell Tissue Kinet*. 3: 393-403.

Grounds MD, White JD, Rosenthal N, Bogoyevitch MA. (2002) The role of stem cells in skeletal and cardiac tissue repair. *J Histochem Cytochem*. 50(5): 589-610.

Gupta N, Su X, Popov B, Lee JW, Serikov V, Matthay MA. (2007) Intrapulmonary delivery of bone marrow-derived mesenchymal stem cells improves survival and attenuates endotoxin-induced acute lung injury in mice. *J Immunol*. 179: 1855–1863.

Hasan W, Pedchenko T, Krizan-Agbas D, Baum L, Smith PG. (2003) Sympathetic neurons synthesize and secrete pro-nerve growth factor protein. *J Neurosci*. 57:38-53.

Hawke TJ, Garry DJ. (2001) Myogenic satellite cells: physiology to molecular biology. *J Appl Physiol*. 91: 534-551.

Iwata Y, Ozaki N, Hirata H, Sugiura Y, Horii E, Nakao E Tatebe M, Yazaki N, Hattori T, Majima M, Ishiguro N. (2006) Fibroblast growth factor-2 enhances functional recovery of reinnervated muscle. *Muscle Nerve*. 34: 623-630.

Izadpanah R, Trygg C, Patel B, Kriedt C, Dufour J, Gimble JM, Bunnell BA.(2006) Biologic properties of mesenchymal stem cells derived from bone marrow and adipose tissue. *J Cell Biochem*. 99: 1285-1297.

Jansen JKS, Lomo T, Nicolaysen K, Westgaard RH. (1973) Hyperinnervation of skeletal muscle fibers: dependence on muscle activity. *Science.* 181: 559-561.

Javernick MA, Doukas WC. (2006) Process for care of battle casualties at Walter Reed Army Medical Center: part I. orthopedic surgery service. *Military Med*. 171(3): 200.

Kang H, Tian L, Thompson W. (2003) Terminal schwann cells guide the reinnervation of muscle after nerve injury. *J Neurocyt*. 32: 975-985.

Kjorstad R, Starnes BW, Arrington E, Devine JD, Andersen CA, Rush RM. (2007) Application to the mangled extremity severity score in a combat setting. *Military Med*. 172(7): 777.

Kragh JF, Svoboda SJ, Wenke JC, Ward JA, Walters TJ. (2005) Epimysium and perimysium in suturing in skeletal muscle lacerations. *J Trauma*. 59: 209.

Kochupura PV, Azeloglu EU, Kelly DJ, Doronin SV, Badylak SF, Krukenkamp IB, Cohen IS, Gaudette GR. (2005) Tissue-engineered myocardial patch derived from extracellular matrix provides regional mechanical function. *Circulation*. 112(9S): I144-I149.

Kuroda R, Usas A, Kubo S, Corsi K, Peng H, Rose T, Cummins J, Fu FH, Huard J. (2006) Cartilage repair using bone morphogenic protein 4 and muscle-derived stem cells. *Arthritis Rheum*. 54(2): 433-442.

Lavasani M, Lu A, Peng H, Cummins J, Huard J. (2006) Nerve growth factor improves the muscle regeneration capacity of muscle stem cells in dystrophic muscle. *Gene Ther*. 17: 180-192.

Lee RH, Kim B, Choi I, Kim I, Choi HS, Suh K, Bae YC, Jung JS. (2004) Characteristic expression analysis of mesenchymal stem cells from human bone marrow and adipose tissue. *Cell Physiol Biochem*. 14(4-6): 311-324.

Li X, Zhu L, Chen X, Fan M. (2007) Effects of hypoxia on proliferation and differentiation of myoblasts. *Med Hypotheses*. 59: 629-636.

Lin DL, Kirk KL, Murphy KP, McHale KA, Doukas WC. (2004) Orthopedic injuries during Operation Enduring Freedom. *Military Med*: 196(10): 807.

Merritt EK, Hammers DW, Tierney MT, Suggs LJ, Walters TJ, Farrar RP. (2009) Functional assessment of skeletal muscle regeneration utilizing homologous extracellular matrix as scaffolding. *Tissue Eng*. Under review.

Mizuno H, Zuk PA, Zhu M, Lorenz HP, Benhaim P, Hedrick MH. (2002) Myogenic differentiation by human processed lipoaspirate cells. *Plast Reconstr Surg*. 109: 199-209.

Murayama T, Tepper OM, Silver M, Ma H, Losordo DW, Isner JM, Asahara T, Kalka C. (2002) Determination of bone marrow-derived endothelial progenitor cell significance in angiogenic growth factor-induced neovascularization in vivo. *Exp Hematol*. 30: 967-972.

Nesti LJ, Jackson WM, Shanti RM, Koehler SM, Aragon AB, Baily JR, Sracic MK, Freedman BA, Giuliani JR, Tuan RS. (2008) Differentiation potential of multipotent progenitor cells derived from war-traumatized muscle tissue. *J Bone Joint Surg Am*. 90: 2390-2398.

Ohtaki H, Ylostalo JH, Foraker JE, Robinson AP, Reger RL, Shioda S, Prockop DJ. (2008) Stem/progenitor cells from bone marrow decrease neuronal death in global ischemia by modulation of inflammatory/immune responses. *Proc Natl Acad Sci USA*. 105(38): 14638–14643.

Owens BD, Wenke JC, Svoboda SJ, White DW. (2006) Extremity trauma research in the United States Army. *J Amer Acad Orthoped Surg*. 14(10): S37-S40.

Padoin AV, Braga-Silva J, Martins P, Rezende K, Rezende ARR, Grechi B, Gehlen D, Machado DC. (2008) Sources of processed lipoaspirate cells: influence of donor site on cell concentration. *Plast Reconstr Surg*. 122(2): 614-618.

Palermo AT, LaBarge MA, Doyonnas R, Pomerantz J, Blau HM. (2005) Bone marrow contribution to skeletal muscle: a physiological response to stress. *Develop Bio*. 279: 336-344.

Payne Jr SH, Brushart TM. (1997) Neurotization of the rat soleus muscle: a quantitative analysis of reinnervation. *J Hand Surg*. 22A: 640-643.

Pittenger MF, Mackay AM, Beck SC, Jaiswal RK, Douglas R, Mosca JD, Moorman MA, Schaffler A, Buchler C. (2007) Concise review: adipose tissue-derived stromal cells – basic and clinical applications for novel cell-based therapies. *Stem Cells*. 25: 818-827.

Prockop DJ. (2009) Repair of tissues by adult stem/progenitor cells (MSCs): controversies, myths, and changing paradigms. *Mol Ther*. 17(6): 939-946.

Qu-Petersen Z, Deasy B, Jankowski R, Ikezawa M, Cummins J, Pruchnic R, Myringer J, Cao B, Gates C, Wernig A, Huard J. (2002) Identification of a novel population of muscle stem cells in mice: potential for muscle regeneration. *J Cell Biol*. 157(5): 851-864.

Rudnicki MA, Schnegelsberg PNJ, Stead RH, Braun T, Arnold HH, Jaenisch R. (1993) MyoD or Myf-5 is required for the formation of skeletal muscle. *Cell*. 75(7): 1351-1359.

Sabourin LA, Rudnicki MA. (2000) The molecular regulation of myogenesis. *Clin Genet*. 57: 16-25.

Simonetti DW, Craig S, Marshak DR. (1999) Multilineage potential of adult human mesenchymal stem cells. *Science*. 284: 143-147.

Strochlic L, Cartaud A, Cartaud J. (2005) The synaptic muscle-specific kinase (MuSK) complex: new partners, new functions. *Bioessays*. 27: 1129-1135.

Takahashi K, Tanabe K, Ohruki M, Narita M, Ichisaka T, Tomoda K, Yamanaka S. (2007) Induction of pluripotent stem cells from adult human fibroblasts by defined factors. *Cell*. 131(5): 861-872.

Tamaki T, Uchiyama Y, Okada Y, Ishikawa T, Sato M, Akatsuka A, Asahara T. (2005) Functional recovery of damaged skeletal muscle through synchronized vasculogenesis, myogenesis, and neurogenesis by muscle-derived stem cells. *Circulation*. 112: 2857-2866.

Teixeira CFP, Zamuner SR, Zuliani JP, Fernades CM, Cruz-Hoffing MA, Fernandes I, Chaves F, Gutierrez JM. (2003) Neutrophils do not contribute to local tissue damage, but play a key role in skeletal muscle regeneration, in mice injected with Bothrops asper snake venom. *Muscle Nerve*. 23: 449-459.

Thomson JA, Itskovitz-Eldor J, Shapiro SS, Waknitz MA, Swiergiel JJ, Marshall VS, Jones JM. (1998) Embryonic stem cell lines derived from human blastocysts. *Science*. 282(5391): 1145-1147.

Tidball JG. (2005) Inflammatory process in muscle injury and repair. *Am J Physiol Regul Integr Comp Physiol*. 288: 345-353.

Till JE, McCullough EA. (1961) A direct measurement of the radiatin sensitivity of normal mouse bone marrow cells. *Radiat Res*. 14: 213–222.

Tu YK, Yen CY, Ma CH, Yu SW, Chou YC, Lee MS, Ueng SWN. (2008) Soft tissue injury management and flap reconstruction for mangled lower extremities. *Injury*. 39;S4: 75-95.

Turrini P, Gaetano C, Antonelli A, Capogrossi MC, Aloe L. (2002) Nerve growth factor induces angiogenic activity in a mouse model of hindlimb ischemia. *Neurosci Let*. 323: 109-112.

Valenzuela DM, Stitt TN, DiStefano PS, Rojas E, Mattsson K, Compton DL, NuSez L, Park JS, Stark JL, Gies DR, Thomas S, Le Beau MM, Fernald AA, Copeland NG, Jenkins NA, Burden SJ, Glass DJ, Yancopoulos GD. (1995) Receptor tyrosine kinase specific for the skeletal muscle lineage: expression in embryonic muscle, at the neuromuscular junction, and after injury. *Neuron*. 15: 573-584.

Wagers AJ, Conboy IM. (2005) Cellular and molecular signatures review of muscle regeneration: current concepts and controversies in adult myogenesis. *Cell*. 122: 659-667.

Walden DL, McCutchan HJ, Enquist EG, Schwappach JR, Shanley PF, Reiss OK, Terada LS, Leff JA, Repine JE. (1990) Neutrophils accumulate and contribute to skeletal muscle dysfunction after ischemia-reperfusion. *Am J Physiol Heart Circ Physiol*. 259: H1809-H1812.

Wang J, Ding F, Gu Y, Liu J, Gu X. (2009) Bone marrow mesenchymal stem cells promote cell proliferation and neurotrophic function of schwann cells in vitro and in vivo. *Brain Res*. 1262: 7-15.

Zammit PS, Beauchamp JR. (2001) The skeletal muscle satellite cell: stem cell or son of stem cell? *Differentiation*. 68: 193-204.

Zheng M, Cao B, Li G, Huard J. Mouse adipose-derived stem cells undergo multilineage differentiation in vitro but primarily osteogenic and chondrogenic differentiation in vivo. *Tissue Eng*. 12(7): 1891-1901, 2006.

Zuk PA, Zhu M, Ashjian P, De Ugarte DA, Huang JI, Mizuno H, Alfonso ZC, Fraser JK, Benhaim P, Hedrick MH. Human adipose tissue is a source of multipotent stem cells. *Mol Biol Cell*. 13: 4279-4295, 2002.

Zuk PA, Zhu M, Mizuno H, Huang J, Futrell JW, Katz AJ, Benhaim P, Lorenz P, Hedrick MH. Multilineage cells from human adipose tissue: implications for cell-based therapies. *Tissue Eng*. 7(2): 211-226, 2001.

VITA

Matthew Timothy Tierney was born in Medina, New York on May 22nd, 1984, the son of Timothy Matthew Tierney and LuAnn Millis Tierney. After completing his work at Medina High School, Medina, New York, in 2002, he entered the University of Rochester in Rochester, New York. He received the degree of Bachelor of Science in chemical engineering from the University of Rochester in May of 2006. In September of 2006, he entered the Graduate School at the University of Texas at Austin.

Permanent Address: 13250 West Lee Road
Albion, NY 14411-9235

This thesis was composed by Matthew T. Tierney.